Geomorphology 116 (2010) 246–263

Contents lists available at ScienceDirect

Geomorphology

journal homepage: www.elsevier.com/locate/geomorph

The implications of geology, soils, and vegetation on landscape morphology: Inferences from semi-arid basins with complex vegetation patterns in Central New Mexico, USA

Omer Yetemen [a,*,1], Erkan Istanbulluoglu [a,2,3], Enrique R. Vivoni [b,c]

[a] Department of Civil and Environmental Engineering, University of Washington, Seattle, WA 98195, USA
[b] School of Earth and Space Exploration, Arizona State University, Tempe, AZ, 85287, USA
[c] School of Sustainable Engineering and the Built Environment, Arizona State University, Tempe, AZ, 85287, USA

ARTICLE INFO

Article history:
Received 1 June 2009
Received in revised form 21 October 2009
Accepted 23 November 2009
Available online 1 December 2009

Keywords:
Geomorphology
Ecogeomorphology
Ecohydrology
Paleoecology
Landscape morphology
Vegetation dynamics

ABSTRACT

This paper examines the relationship between land surface properties (e.g. soil, vegetation, and lithology) and landscape morphology quantified by the catchment descriptors: the slope–area (S–A) relation, curvature–area (C–A) relation, and the cumulative area distribution (CAD), in two semi-arid basins in central New Mexico. The first site is composed of several basins located in today's desert elevations with mesic north-facing and xeric south-facing hillslopes underlain by different lithological formations. The second site is a mountainous basin exhibiting vegetation gradients from shrublands in the lower elevations to grasslands and forests at higher elevations. All three land surface properties were found to have significant influences on the S–A and C– A relations, while the power-law exponents of the CADs for these properties did not show any significant deviations from the narrow range of universal scaling exponents reported in the literature. Among the three different surface properties we investigated, vegetation had the most profound impact on the catchment descriptors. In the S–A diagrams of the aspect-controlled ecosystems, we found steeper slopes in north-facing aspects than south-facing aspects for a given drainage area. In elevation-controlled ecosystems, forested landscapes exhibited the steepest slopes for the range of drainage areas examined, followed by shrublands and grasslands in all soil textures and lithologies. In the C–A diagrams, steeper slopes led to a higher degree of divergence on hillslopes and a higher degree of convergence in the valleys than shallower slopes. The influence of functional types of vegetation detected on observed topography provided some initial understanding of the potential impacts of life on the organization of topography. This finding also emphasizes the critical role of climate in catchment development. We suggest that climatic fluctuations that are capable of replacing vegetation communities could lead to highly amplified hydrological and geomorphic responses.

Published by Elsevier B.V.

1. Introduction

Topography emerges from the competition of various geomorphic processes under the influence of land surface properties such as rock type, soils, and vegetation. Each of these properties vary naturally in space and time and may lead to differential catchment erosion, resulting in differences in the observed morphology of landscapes (Hancock, 2005; Dietrich and Perron, 2006; Cohen et al., 2008). Whereas rock type may be treated as a constant landscape variable over geomorphically significant time scales, it is arguable that soil and vegetation co-evolve with topography under a changing climate through weathering–erosion–deposition cycles and strong interactions with bedrock (Lavee et al., 1998; Waters and Haynes, 2001; Bierman et al., 2005; Monger and Bestelmeyer, 2006; Buxbaum and Vanderbilt, 2007). The role of rock strength on hillslope and basin relief (Schmidt and Montgomery, 1995, 1996) as well as channel profile properties and rates of channel incision (Stock and Montgomery, 1999; Whipple, 2004; Stock et al., 2005) have long been discussed. Little is known, however, about the role of parent material on different process domains within soil-mantled landscapes under the varying influence of soil production and vegetation dynamics.

Soil development over rock is a precondition for the establishment of soil flora and fauna where climate permits. Once established, biota shifts the form of the dominant soil transport mechanisms from physical (Gabet, 2003) to biotic processes on hillslopes (e.g., Gabet, 2000; Gabet et al., 2003). Recent research further demonstrates how

* Corresponding author. 201 More Hall, Box 352700, Dept. of Civil and Environmental Engineering, University of Washington, Seattle, WA 98195-2700, USA. Tel.: +1 206 543 7923; fax: +1 206 543 1543.
E-mail address: yetemen@u.washington.edu (O. Yetemen).
[1] Formerly at Department of Geosciences, University of Nebraska-Lincoln, Lincoln, NE, 68588, USA.
[2] Formerly at School of Natural Resources, University of Nebraska-Lincoln, Lincoln, NE, 68583, USA.
[3] Formerly at Department of Biological Systems Engineering, University of Nebraska-Lincoln, Lincoln, NE, 68583, USA.

0169-555X/$ – see front matter. Published by Elsevier B.V.
doi:10.1016/j.geomorph.2009.11.026

strongly biota alters the type and magnitude of sediment transport on hillslopes (Yoo et al., 2005; Roering, 2008) and in channels (Montgomery et al., 1996; Murray and Paola, 2003; Lancaster and Grant, 2006). Soil formation and the establishment of vegetation also dramatically changes hydrological fluxes by accommodating soil moisture and facilitating the formation of subsurface flow paths (Torres et al., 1998; Montgomery and Dietrich, 2002; Montgomery et al., 2002; Ebel et al., 2007a). These soil and vegetation related alterations in hydrology strongly impact the form and magnitude of erosion, sediment transport (Casadei et al., 2003; Ebel et al., 2007b), and deposition (Molina et al., 2009) across the landscape. As a consequence, numerical models of landscape evolution predict a strong dependence of simulated landscape features to mechanisms generating runoff (Ijjász-Vásquez et al., 1992; Tucker and Bras, 1998; Bogaart et al., 2003), soil and vegetation properties (Casadei et al., 2003; Collins et al., 2004; Istanbulluoglu and Bras, 2005), climate change (Rinaldo et al., 1995; Tucker and Slingerland, 1997), and spatial variability of landscape erodibility (Moglen and Bras, 1995a,b; Gasparini et al., 2004), and show how such differences may be captured by some quantitative catchment descriptors including the slope–area relation and the cumulative area distribution.

While these model predictions offer testable hypothesis for natural landscapes, little has been done to relate the observed landscape morphology to lithology, soils, and vegetation at the basin scale. Some earlier efforts sought connections between hillslope form and spatial patterns of land surface properties in the opposing hillslope aspects in semi-arid climates. These include comparison of aspect-related differences on the morphology of badland slopes (Churchill, 1981) and terrace scarps (Pierce and Colman, 1986). Generally, in soil-mantled landscapes of the northern hemisphere, wetter north-facing slopes were found to be steeper than south-facing slopes, attributed to the denser vegetation cover on north-facing slopes that restrain runoff erosion (Hadley, 1961; Branson and Shown, 1989; Istanbulluoglu et al., 2008). This observation, however, is often reversed in rock slopes where physical weathering processes outpace bioturbation. In a series of small weathering-limited valleys, Smith (1978) documented steeper southwest- and northeast-facing slopes than those of other aspects and attributed this observation to differential rates of weathering in combination with diurnal cycles of moisture retention and rapid heating and cooling. Recently, Burnett et al. (2008) documented steeper south-facing slopes than north-facing slopes in canyon walls of semi-arid northern Arizona. In their field site, Burnett et al. (2008) proposed higher rates of weathering of clay minerals on wetter north-facing slopes as a plausible mechanism leading to shallower north-facing slopes.

At the basin scale, Hancock (2005) demonstrated notable impacts of lithology on some catchment geomorphic descriptors such as the slope–area relation, the cumulative area distribution, and basin hypsometric distribution. His analysis also revealed that catchments with heterogeneous lithology have longer hillslopes than their homogeneous counterparts. In addition to lithology, Cohen et al. (2008) related the spatial variability of types of soils to catchment geomorphic descriptors used by Hancock (2005) and others. They argued that at a subcatchment scale the slope–area relation is closely linked to types of soils observed in the field, and presented a new methodology for explicit calculation of the empirical parameters of the slope–area relation at a pixel scale.

The aforementioned studies provide a preliminary empirical basis for the following related questions that remain to be tackled in quantitative geomorphology: (1) How do soils and biota interact with climate and bedrock, and modulate the geomorphic response of a catchment? (2) How do soils and biota alter the time scales of whole landscape geomorphic response? and (3) How will global warming impact sediment yields and landscape form in relation to projected changes in the ecosystem? One way to address these questions empirically is to investigate the associations between the properties of the land surface and topography by conducting spatial analysis of digital maps of elevation, geology, soils, and vegetation in relation to the regional climate history and records of sediment yield. For this purpose, we studied semi-arid landscapes in central New Mexico (USA), where hillslope aspect and elevation control the structure of the ecosystem. The slope–area relationship, the curvature–area relationship, and the cumulative distribution of contributing areas are used as quantitative catchment geomorphic descriptors. This paper builds on some of the earlier findings of Istanbulluoglu et al. (2008) in an aspect-controlled ecosystem in central New Mexico.

2. Study areas

This study was conducted using two study areas in central New Mexico, with ecosystems characterized by aspect and elevation control.

2.1. Study area for the aspect-controlled ecosystems

We examined the role of lithology and aspect on geomorphic descriptors in eight catchments (1.8 km^2–12 km^2 in size) located at the foot of the Ladron Peak in the northwestern corner of the SNWR (Sevilleta Wildlife National Refuge) in central New Mexico (Fig. 1a and b), with hillslopes primarily oriented north and south (McMahon, 1998; Gutiérrez-Jurado et al., 2006, 2007). Catchments used in this study are within an elevation range of 1500 m–1900 m. Mean annual precipitation in the region is approximately 250 mm, and ~50% of this precipitation occurs during the North American monsoon (July to September) (Vivoni et al., 2008). Vegetation is distinctly different between the wetter north- and drier south-facing slopes (Dickie-Peddie, 1993; Gutiérrez-Jurado et al., 2007). The north-facing slopes are typically mesic ecosystems with one-seed Juniper (*Juniperus monosperma*) and dense black grama (*Bouteloua eriopoda*), and deeper soils with higher organic matter, $CaCO_3$, silt and clay contents. The south-facing slopes are xeric ecosystems comprised primarily of creosote bush (*Larrera tridentata*), and sparser fluff grass (*Erioneuron pulchellum*) (McMahon, 1998; Gutiérrez-Jurado et al., 2007). In addition, north-facing slopes are slightly steeper and longer than south-facing slopes, and have planar mid-slopes with rounded and smoother ridges (Fig. 1c). South-facing slopes on the other hand are typically dissected by rills and gullies (Fig. 1d).

Two units of the Sante Fe Group characterize the geology of the selected catchments: the early Pliocene to middle Pleistocene aged the Sierra Ladrones Formation (SLF), consisting of alluvial fan, piedmont slope, floodplain, and axial stream deposits; and early to late Miocene aged the Popotosa Formation (PF). The PF is the deepest unit within the Santa Fe Group, and is typically overlain by the SLF (Bruning, 1973; Green and Jones, 1997).

Because of the dominant control of aspect on the spatial distribution of vegetation and soils in the region (e.g., McMahon, 1998; Gutiérrez-Jurado et al., 2006, 2007), we use aspect as a surrogate variable for ecosystem classification. We classified north, northwest, and northeast aspects as north-facing mesic ecosystems; and south, southeast, and southwest slopes as south-facing xeric ecosystems. East- and west-facing hillslopes are not considered here as these typically contain the boundaries between the two opposing ecosystems. This classification is also adopted because the publicly available digital data sets with ~30 m spatial resolution for soils (e.g., US Department of Agriculture, STATSGO) and vegetation (National Land Cover Data, NLCD) cannot adequately distinguish the observed spatial structure of the soils and the ecosystem in these desert elevation of the central New Mexico.

To examine the influence of lithology and aspect on relatively homogeneous surface conditions, we selected seven basins that are individually underlain by the same lithology (either PF or SLF) and have relatively small elevation differences. Four basins were selected to represent the SLF (Qts/Qtf) (Fig. 1b). Among these, three basins are

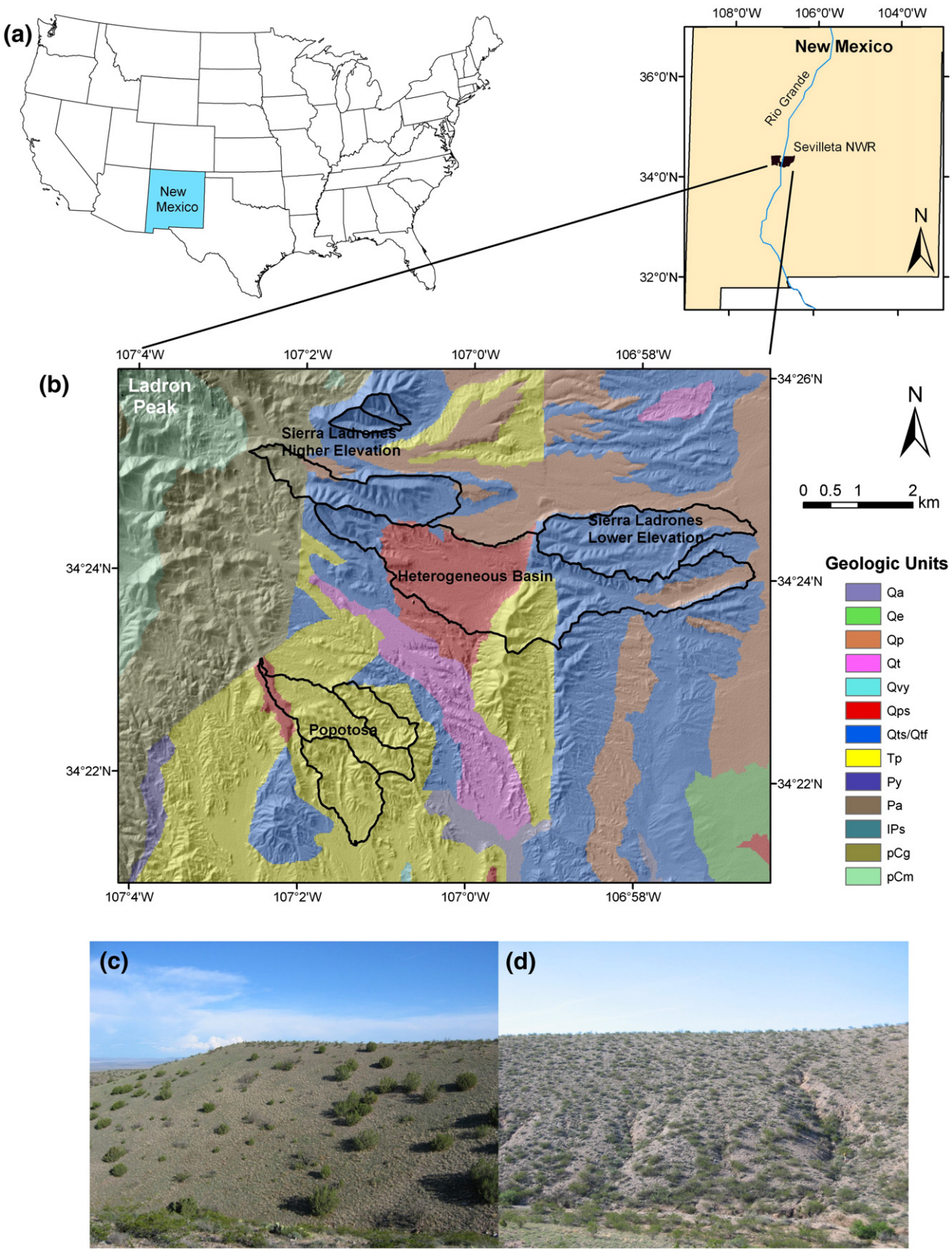

Fig. 1. (a) Location map; (b) geology map and the watershed boundaries of the catchments in the Sevilleta National Wildlife Refuge (SNWR) in central New Mexico; (c) a north-facing piñon-juniper and grassland savanna ecosystem with planar hillslope profile; (d) a dissected south-facing slope experiencing active hollow formation through ephemeral gully incision.

located at a higher elevation range (1711 m to 1920 m), and one at a lower elevation range (1567 m to 1711 m), enabling to investigate the role of elevation on geomorphic descriptors. Throughout the paper, these basins are called the Higher SLF and the Lower SLF, respectively. Three other small basins were selected on the PF (Tp), all between 1628 m and 1789 m elevation (Fig. 1b). In addition to seven homogeneous basins, we selected a basin composed of different lithologies to examine the influence of geologic heterogeneity on the geomorphic descriptors used in this study. This basin is composed of the piedmont-slope facies of the SLF in its headwaters (Qps), Tp and Qts/Qtf in the middle, and valley border alluvium (Qp) near the outlet, with an elevation range of 1566 m–1907 m (Fig. 1b). A 10-m digital elevation model (DEM) derived from Interferometric Synthetic Aperture Radar (IfSAR) is used to derive the local slope, aspect, drainage area, and curvature fields in the basins.

2.2. Study area for the elevation-controlled ecosystems

We examined the role of lithology, soil, and types of vegetation on geomorphic descriptors in the Upper Rio Salado (URS) basin. The URS basin is located in the Colorado Plateau physiographic region in west-central New Mexico, 70 km west of the SNWR. The basin covers an area of 464 km^2 within an elevation range of 1985 m to 2880 m. Annual rainfall for the growing season varies between 220 mm at lower, and 325 mm at higher elevations of the URS (Caylor et al., 2005; Vivoni et al., 2009). The location, DEM, geology, soil, and vegetation maps of the basin are presented in Fig. 2.

Two geologic units, including the Crevasse Canyon Formation (Kcc) from Upper Cretaceous, and the Paleogene sedimentary units (Tps) form the dominant lithology in the basin (Fig. 2c) (New Mexico Bureau of Geology and Mineral Resources, 2003). The Quaternary alluvium (Qa) largely underlies the main channel. The Kcc covers majority of the lower elevations, followed by the Tps as elevation increases. Middle Tertiary, Oligocene and upper Eocene, sedimentary and volcaniclastic sedimentary rocks (Tvs) are located on the southern boundaries of the study site. Kgm, from upper Cretaceous, represents Gallup sandstone isolated in the lower elevations of the northeastern part of the basin close to the main stem of the river. Lower Oligocene to upper Eocene aged Tlrp represents pyroclastic rocks and ash-flow tuffs of the Datil Group located through the southeastern edges of the study area.

The soil texture information is obtained from the United States Department of Agriculture (USDA) STATSGO database (Soil Survey Staff, 1994). Soil textures in the URS basin include sandy loam, silt loam, and loam. Silt loam and loam have similar surface areas. Silt loam makes up the majority of the northern tributaries, some of which have sandy loam valley bottoms (Fig. 2d). The south-facing tributaries and the higher elevations of north-facing tributaries are covered by loam.

The 1992 National Land Cover Data (NLCD) (28.5 m grid resolution) is used to identify vegetation patterns in the basin (Vogelmann et al., 2001). The NLCD vegetation map was previously used for ecohydrological analysis in the URS (Caylor et al., 2005). Types of vegetation are greatly impacted by elevation. Shrubs, primarily creosote bush (*Larrea tridentata*), dominate the lowlands (1985 m–2075 m); a combination of grasses (galleta, *Hilaria jamesii* and blue grama, *Bouteloua gracilis*) and shrubs cover the mid-elevations (2075 m–2250 m); and forests (woodlands of piñon pine, *Pinus edulis*; and one-seed juniper, *Juniperus monosperma*) cover the upper elevations (2250 m–2880 m) (Dickie-Peddie, 1993; Caylor et al., 2005) (Fig. 2e).

3. Methods: Quantitative measures of catchment morphology

3.1. Slope–area (S–A) relation

A power-law relationship between the local slope of a given point on the landscape and its contributing area in the form: $S = k \cdot A^{\theta}$, is widely observed in natural landscapes. In channels, k and θ are referred to as the steepness index and the concavity index, respectively. The concavity index is the gradient (degree of steepness) of the slope–area (S–A) relation in a log–log plot, ($\log(S) = \log(k) + \theta\log(A)$). In fluvial valleys, most θ values fall in the range between -0.4 and -0.7, although values as low as -0.1 are not uncommon for low-relief alluvial systems and badlands (Howard, 1980; Tarboton et al., 1992). This relationship has been widely used to examine the observed and modeled river profiles in relation to process-based theory (Snow and Slingerland, 1987; Sklar and Dietrich, 1998; Whipple and Tucker, 2002; Whipple, 2004; Gasparini et al., 2007), the impacts of variable rock uplift and rates of erosion (Wobus et al., 2006), and landscape relief (Willgoose, 1994).

The parameters of the S–A relation have been related to the dominant form of sediment transport process in the basin, which can be theoretically described by a geomorphic transport law (GTL). In GTLs, sediment detachment and transport are often represented as a function of certain topographic variables (e.g., slope, curvature, drainage area), and constants that implicitly lump together the role of climate, soils, vegetation, and lithology. In transport-limited soil-mantled landscapes with loose sediments, the long-term average transport of sediment can be described by the following generic GTL, which can be used, with proper parameter values, for modeling fluvial and soil creep transport:

$$Q_s = KA^m S^n, \tag{1}$$

where Q_s is sediment flux [MT^{-1}]; A is basin drainage area [L^2], S is local slope [L/L] and K is an empirical transport efficiency coefficient that lumps the influence of climate, vegetation, hydrology, and lithology [MT^{-1} L$^{-2\,m}$]. The parameters m and n vary with different form of erosion (Kirkby, 1971; Montgomery, 2001). For soil creep $m = 0$ leading to a slope-dependent GTL for hillslopes. Fluvial processes often take $m > 1$ and $n > 1$. A theoretical basis for the slope–area relation was described as the following (Willgoose et al., 1991; Tarboton et al., 1992). If the long-term average rate of denudation (D) is equal everywhere in the basin, the sediment flux in the basin for a given A is:

$$Q_s = D \cdot A. \tag{2}$$

In a transport-limited landscape, S adjusts to A such that sediment transport capacity is just equal to total sediment flux, leading to a power-law relationship for S (Tarboton et al., 1992):

$$S = kA^{\theta},\ k = \left(\frac{D}{K}\right)^{\frac{1}{n}} \qquad \theta = \frac{(1-m)}{n}. \tag{3}$$

Sediment transport in soil-mantled hillslopes where runoff is not erosive is characterized by a transport-limited slope-dependent diffusive process with $m = 0$. This leads to a positive relationship between S and A ($\theta > 0$), suggesting a convex hillslope morphology (e.g., McKean et al., 1993). For fluvial sediment transport, m and $n > 1$, in which case (3) predicts an inverse relationship for S with A ($\theta < 0$), representing a concave upward channel profile. Some degree of dependence of these process coefficients on vegetation properties (Gabet and Dunne, 2003; Istanbulluoglu and Bras, 2005), soils (Cohen et al., 2008), and geology (Moglen and Bras, 1995a,b; Hancock, 2005) have been proposed.

3.2. Curvature–area (C–A) relation

Corollary to the slope–area scaling, landscape curvature (i.e. Laplacian of elevation z, $\nabla^2 z$) is another useful measure for the interpretation of dominant sediment transport processes on the landscape (Bogaart and Troch, 2006; Istanbulluoglu et al., 2008;

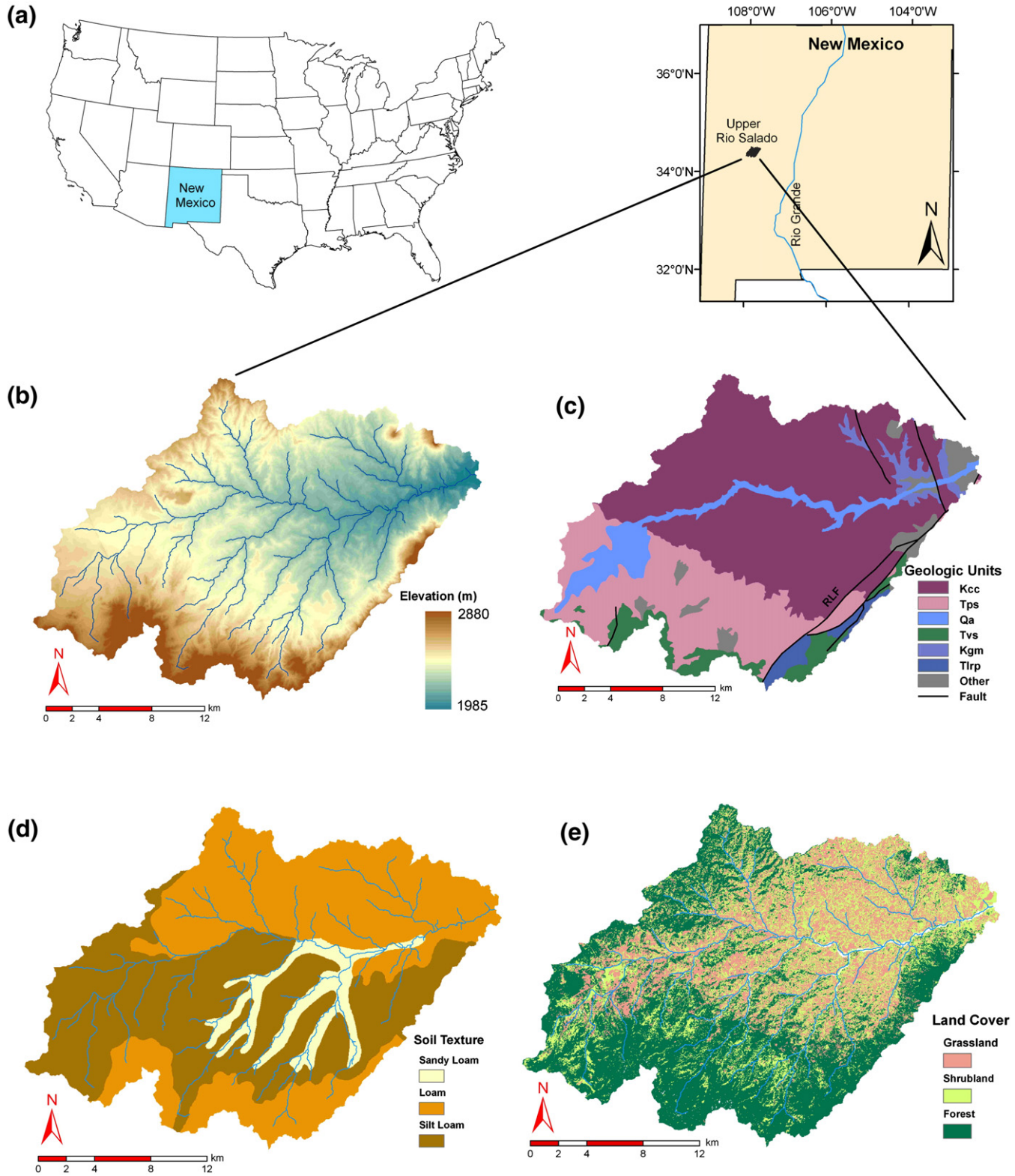

Fig. 2. (a) Location; (b) elevation; (c) geology; (d) soil; and (e) vegetation maps of the Upper Rio Salado (URS) basin in central New Mexico.

Tarolli and Dalla Fontana, 2009). Total curvature is defined as the sum of planform ($\partial^2 z/\partial x^2$) and profile ($\partial^2 z/\partial y^2$) curvatures:

$$\nabla^2 z = \left(\frac{\partial^2 z}{\partial x^2} + \frac{\partial^2 z}{\partial y^2}\right) \tag{4}$$

Planform curvature represents the degree of divergence or convergence perpendicular to flow direction. Profile curvature represents the convexity or concavity along the flow direction. In general terms, divergent-convex landforms ($\nabla^2 z<0$) are formed by hillslope diffusion, while concave-convergent landforms ($\nabla^2 z>0$) result from fluvial sediment transport.

3.3. Cumulative area distribution (CAD)

As the third quantitative measure, we used the cumulative distribution of contributing areas in the form of an exceedance plot, calculated as: $P(A \geq \alpha) = n/N$, where n is the number of pixels with contributing area greater than or equal to a selected contributing area, a, and N is the total number of pixels in the basin. This distribution was pioneered by Rodríguez-Iturbe et al. (1992) to examine the aggregation structure of river basins, who showed that the shape of the distribution on a log–log plot forms a straight line following a power-law equation as:

$$P(A \geq a) \propto a^{-\beta} \quad (5)$$

where, β is scaling exponent often ~0.43 regardless of the type of climate, vegetation, soil, and rock that form the river network (Rodríguez-Iturbe et al., 1992).

4. Results

4.1. Landform analyses in aspect-controlled ecosystems

First, we use the geomorphic catchment descriptors to investigate relations between landscape morphology and lithology in the SNWR basins. This step is critical to illustrate the background control of lithology at the basin scale before analyzing the role of soils and vegetation at the hillslope scale. The slope–area (S–A) and curvature–area (C–A) relations, and the cumulative area distributions (CAD) of the SNWR basins underlain by the SLF (at two different elevation ranges), the PF, and a heterogeneous lithology are given in Figs. 3 and 4, respectively.

The PF slopes are much steeper than the Lower SLF (difference as high as 0.1 m/m) for the entire range of areas plotted, while the heterogeneous basin, a hybrid of both formations as well as one other formation, plots between the two homogeneous lithologies. The PF and Lower SLF basins are within a very close elevation range, share similar vegetation patterns, and climate. Therefore, we treat the observed differences in the S–A relations as an indication of lithological control on basin morphology.

Up to four different scaling regimes may be observed in a S–A relation (Ijjasz-Vasquez and Bras, 1995; Tucker and Bras, 1998; McNamara et al., 2006). Region I with a positive S–A gradient ($\theta > 0$) corresponds to hillslopes with lower drainage areas where sediment is dominantly transported by soil creep. Fluvial transport overwhelms hillslope diffusion in region II (Ijjasz-Vasquez and Bras, 1995). The steepest slopes on the landscape are located in the boundary between region I and II, where diffusive processes give way to fluvial erosion, marking the location of the valley head. The channel head with definable banks often begins somewhere down the valley with greater contributing areas and lower slopes than the valley head

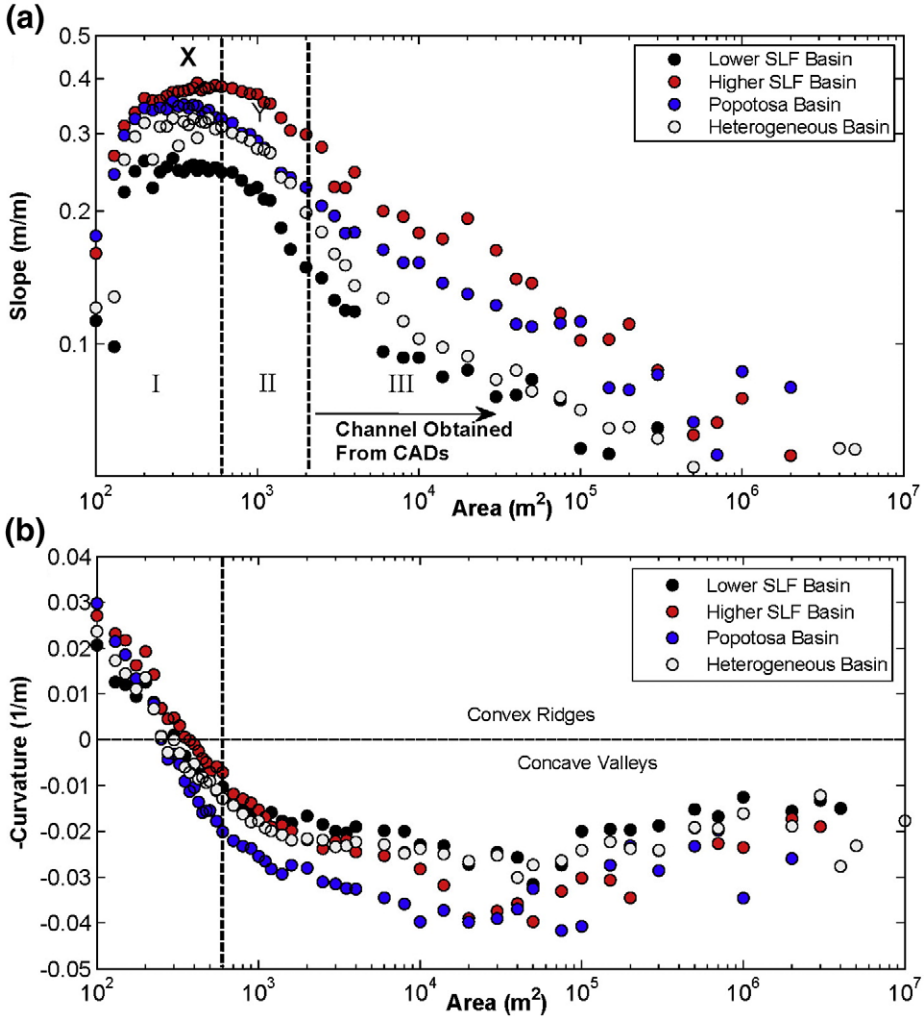

Fig. 3. The slope–area (a) and curvature–area (b) relations for basins grouped with respect to different dominant lithologies. The vertical lines designate approximately the limits of the scaling regions I and II identified for the S–A relation of the Sierra Ladrones Formation (SLF) basins, and the letters X and Y show those for the Popotosa Formation (PF) basin, respectively.

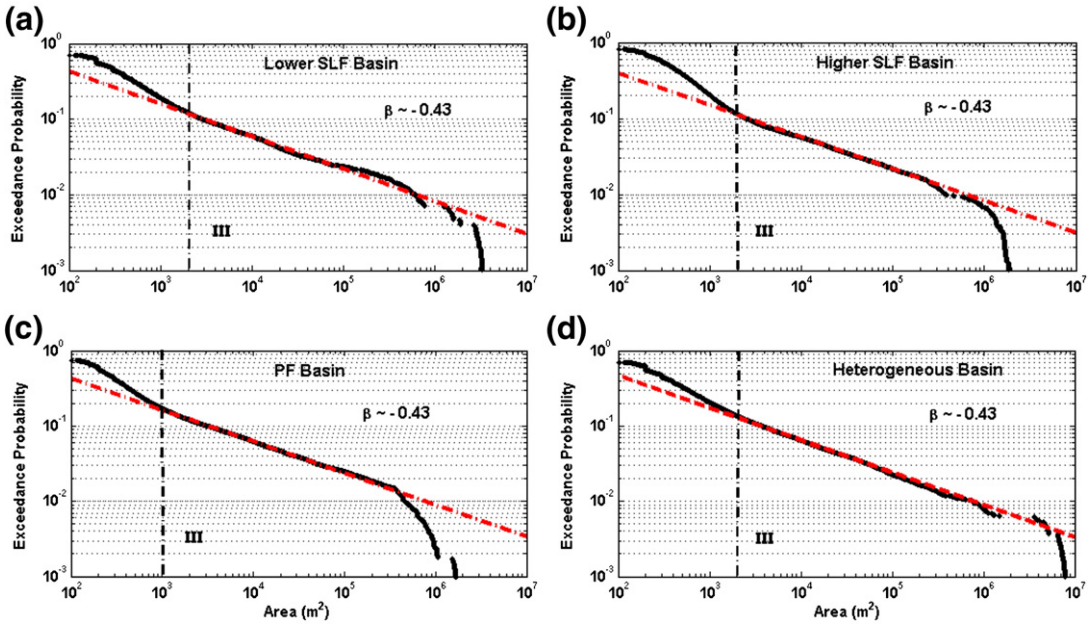

Fig. 4. Cumulative area distribution (CAD) for the SLF lower elevation (a) and higher elevation (b) basins; the PF basin (c); and the heterogeneous basin (d). The vertical line in each plot specifies approximately the area above which a power-law distribution holds, and theoretically designates the channel head support area.

(Montgomery and Foufoula-Georgiou, 1993; Montgomery and Dietrich, 1994). In some landscapes, channels are distinguished by a reduction in the gradient of the S–A relation (Ijjasz-Vasquez and Bras, 1995).

According to the S–A relation in Fig. 3a, valleys begin with a smaller contributing area (~300 m^2, location indicated by X) in the PF basin than the lower SLF basin (~600 m^2, location indicated by a vertical line), while the turnover point of the S–A relation of the heterogeneous basin appears between the two homogeneous counterparts. In all basins, the transitions from hillslopes to valleys are manifested by a change in the sign of landscape curvature (Fig. 3b). This suggests a change of the landscape form from convex to concave topography at the valley head. Interestingly, in each basin, change in the sign of curvature is marked with a smaller contributing area than that identified at the point of slope–area turnover, designated by the vertical line for the SLF basins. This may indicate that profile concavity begins slightly downslope of the point where valley planform becomes converging (Eq. (4)), resulting in a higher drainage area at the S–A turnover.

Based on our experience in this landscape, channels begin farther down the valley head, and, therefore, the S–A turnover in Fig. 3a does not correspond to the location of channel heads (Istanbulluoglu et al., 2008). To identify and compare the channels among different lithologies, first, we look for a reduction in the gradient of the fluvial portion of the S–A relation as reported in the literature (e.g., Ijjasz-Vasquez and Bras, 1995). Although not very clear, some evidence of that exists in all of the SNWR basins except the Higher SLF. To more closely examine and identify channels theoretically, we relate the S–A relation to the CAD of these basins, as the straight portion of a CAD in a log–log domain designates channels (Fig. 4). CADs of the Higher and the Lower SLF and the heterogeneous basins follow a straight line for areas greater than 2×10^3 m^2 (Fig. 4a, b, d), while the straight portion of the distribution for the PF basin begins with a smaller area value ~1000 m^2 (Fig. 4c). The exponent of a power function fitted to the straight portions of the CADs is nearly identical ~0.43, to the universal value of Rodríguez-Iturbe et al. (1992). When demarked on the area axis of Fig. 3a (the vertical line at ~2000 m^2 for SLF basins and the letter Y for the PF basin), however, these area thresholds do not correspond to any direct gradient changes in the S–A relations. This may indicate that, the accumulation structure of channels does not leave a clear signature on the S–A relation of the basins developed from binned average data. It is conceivable that this suggests a transitional topographic state such that the landscape is either responding to changes in the external forcing or still incising the alluvial fan that formed the initial condition to the SNWR basins.

To examine the geomorphic impacts of the observed aspect-dependent ecosystem and soil patterns in the SNWR, next, we constrain the S–A and C–A relations to north- and south-facing slopes of the basins in the SLF (Lower basin in Fig. 5a, c; Higher basin in Fig. 5b, d); the PF (Fig. 5e, g), and the heterogeneous lithology (Fig. 5f, h). The analyses are limited to hillslopes (<0.1 km^2) within the selected basins, as the opposing north and south-facing hillslopes drain into an east-flowing drainage network. Because of that, the comparisons presented in Fig. 5 are largely limited to low-order channels and headwater valleys in the basins studied in the SNWR.

The plots reveal slightly higher north-facing slopes than south-facing slopes (Fig. 5a, b, e, f) across all lithologies and elevation ranges. For the plotted bin ranges, 71% and 61% of the opposing average slopes have different means at $\alpha=0.05$ and $\alpha=0.01$ significance levels, respectively. These subtle but statistically significant differences in slopes are reflected on the C–A relationship. Compared to south-facing slopes, north-facing aspects show slightly higher positive curvature on ridges and higher negative curvature in valleys (Fig. 5c, d, g, h). The differences are statistically significant in 61% ($\alpha=0.05$) and 45% ($\alpha=0.01$) of the plotted average curvature data.

Some distinguishable features also occur in the form of the S–A relation of the opposing slopes. A flat region is apparent in the north-facing slopes of the Lower SLF between ~200 m^2 and ~600 m^2 (Fig. 5a), and Higher SLF between ~300 m^2 and ~1100 m^2 (Fig. 5b). This implies planar hillslope morphologies between these area limits on north-facing slopes, consistent with our field observations in the region (Fig. 1c). On south-facing slopes such a flat region does not exist and the transition from a positive to a negative θ occurs at smaller drainage areas. As in the case of lithological comparisons, aspect-related soils and vegetation differences seem to have a similar impact on the S–A relations, mediating the slope steepness, valley head positions, and the form of hillslope–valley morphology.

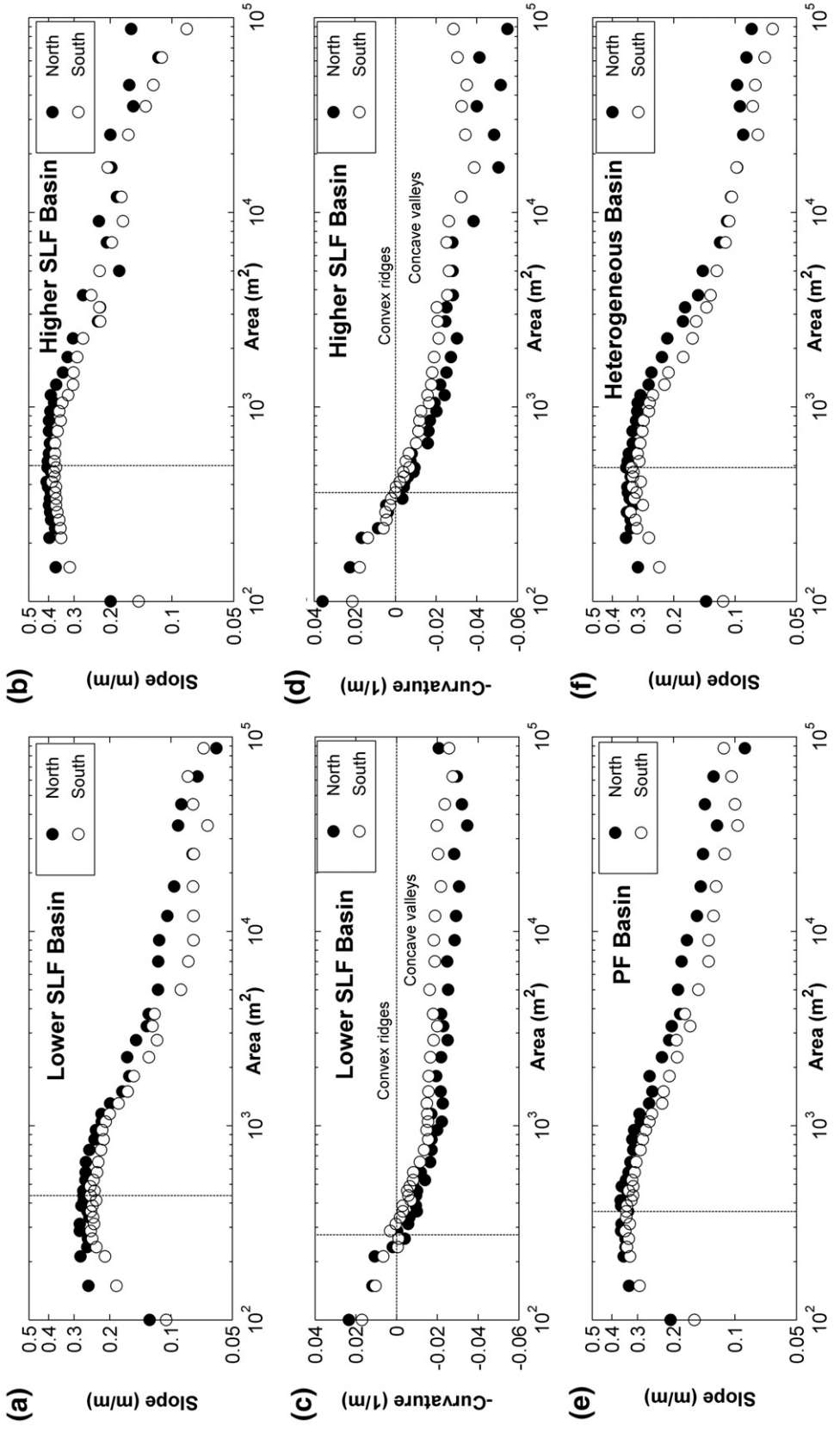

Fig. 5. Slope–area (S–A) and curvature–area (C–A) plots of north- and south-facing slopes of the SLF lower elevation (a, c) and higher elevation (b, d) basins; PF basin (e, g); and the heterogeneous basin (f, h). Vertical dashed lines indicate the approximate location of the valley head on the S–A domain, and the area that corresponds to the change in the sign of curvature in the C–A domain.

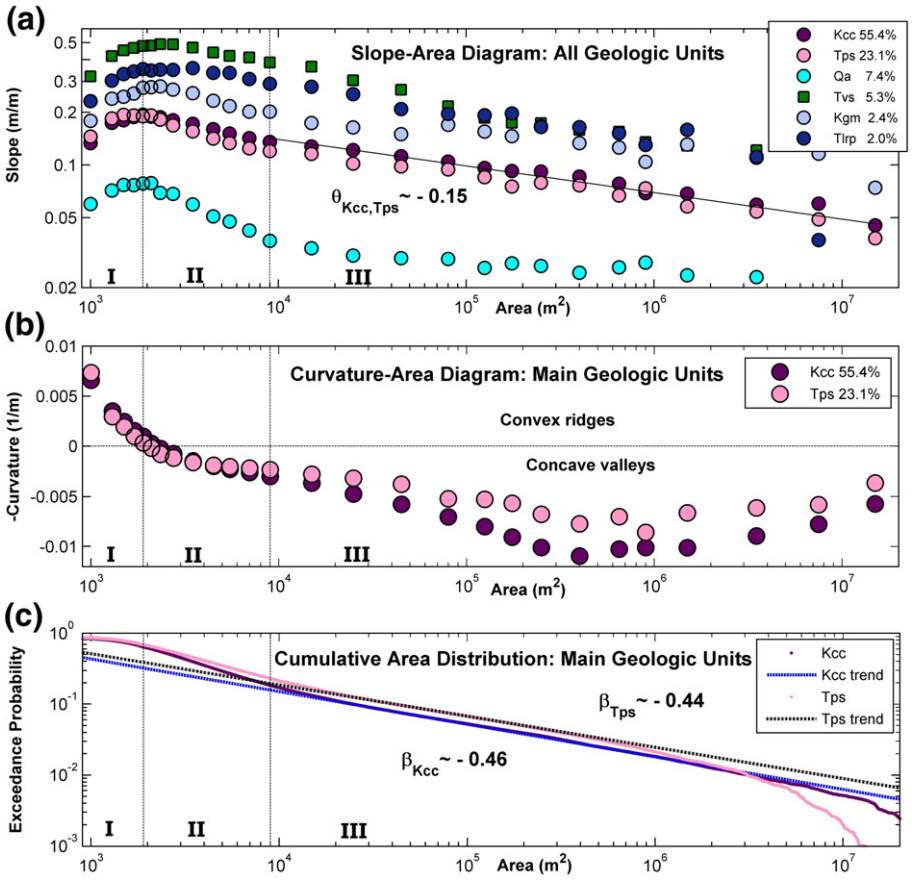

Fig. 6. (a) Slope–area (S–A) relation; (b) curvature–area (C–A) relation and; (c) cumulative area distribution (CAD) of the geologic units in the URS basin.

4.2. Landform analyses in elevation-controlled ecosystems

4.2.1. Individual comparisons of land surface properties and the URS topography

Figs. 6, 7, and 8 illustrate the S–A and C–A relations, and the CAD for the URS basin areas grouped with respect to only lithology, soil, and vegetation, respectively. In all S–A relations, the vertical lines at 900 m^2 and 9000 m^2 designate the three S–A scaling regions, visually defined based on change in the gradient of the S–A relations for Kcc and Tps formations. These formations occupy 55% and 23% of the entire basin area, respectively; while a large fraction of the remaining 22% is occupied by four other lithologies.

A clear separation exists among the S–A relations in Fig. 6a. Erosionally resistant volcaniclastic unit Tvs (Chamberlin et al., 1994), shows the highest slopes in the plotted area range, especially in regions I and II, followed by Tlrp. Both lithologies are located in the southern basin divide at high elevations. In addition to rock strength, the steeper slopes of Tvs and Tlrp lithologies may also be related to fault activity. The Red Lake Fault (see RLF in Fig. 2c) runs through the southeastern boundary of the basin (Chamberlin et al., 1994; Green and Jones, 1997). Stratigraphically located beneath the Kcc formation, the Kgm formation is the third steepest lithology following Tvs and Tlrp, especially in regions I and II. In region III, the S–A relation of the steeper lithologies blend into each other. These altogether cover approximately 9.7% of the basin area. The shallowest slopes in Fig. 6a belong to Qa (Quaternary Alluvium), confined in the main channel and several tributary basins in the headwater regions of the URS basin. It is likely that the highly erodible nature of the non-cohesive alluvial deposits lead to the observed shallow slopes, as in Eq. (4), a higher value of the transport coefficient K leads to a smaller k (steepness index), and as a result, a lower S. Finally, the two dominant lithologies, Kcc and Tps, not directly associated with faulting, show subtle differences in the S–A relations, with an identical concavity index ($\theta \cong -0.15$) in region III.

Next, we discuss the influences of soil texture on catchment descriptors. In the URS basin, loam occupies much steeper regions on the landscape than silt loam and sandy loam (Fig. 7a). Loam areas are dominantly underlain by Kcc and Kgm lithologies in the northern flank of the basin, and Tvs and Tlrp formations in the southern catchment boundary. Because of the underlying resistant lithology and proximity to the RLF, the southern region contributes significantly to the overall steepness of the loam S–A plot. The opposite is true for silt loam which lies in less steep regions that contain Qa and Tps lithologies, resulting in shallower slopes and a smaller concavity index than those of loam. Plotting separately the major rock types that underlie the silt loam surface, we identified that the lower θ is caused by the headwater regions of the main channel dominated by Qa lithology which has a nearly flat S–A relation in region III (Fig. 6a). When this highly erodible region is excluded in the S–A plot of silt loam, θ becomes ~ -0.15 for silt loam underlain by Tps, consistent with loam regions but with shallower slopes (figure not presented).

Following geology and soil texture, we repeat the same analysis for types of vegetation (Fig. 8). The S–A scaling regimes of the three vegetation species can be clearly distinguished from one another in Fig. (8a). For all ranges of areas from ridges to large valleys, forests show the steepest binned average slopes followed by shrubs and grasses, respectively. The S–A relations for areas less than about 0.6 km^2 are approximately parallel on the log–log plot and the transitions between scaling regimes (from I to II, and II to III) occur at approximately identical drainage areas for each type of vegetation. The θ indices of the plotted S–A relations are: $\theta = 0.44$ in region I, $\theta = -0.33$ in region II, and $\theta = -0.16$ in region III. The steepness index, k (Eq. (3)), however, changes from grasslands to forests up to twofold in all regions. From a theoretical standpoint, these findings suggest

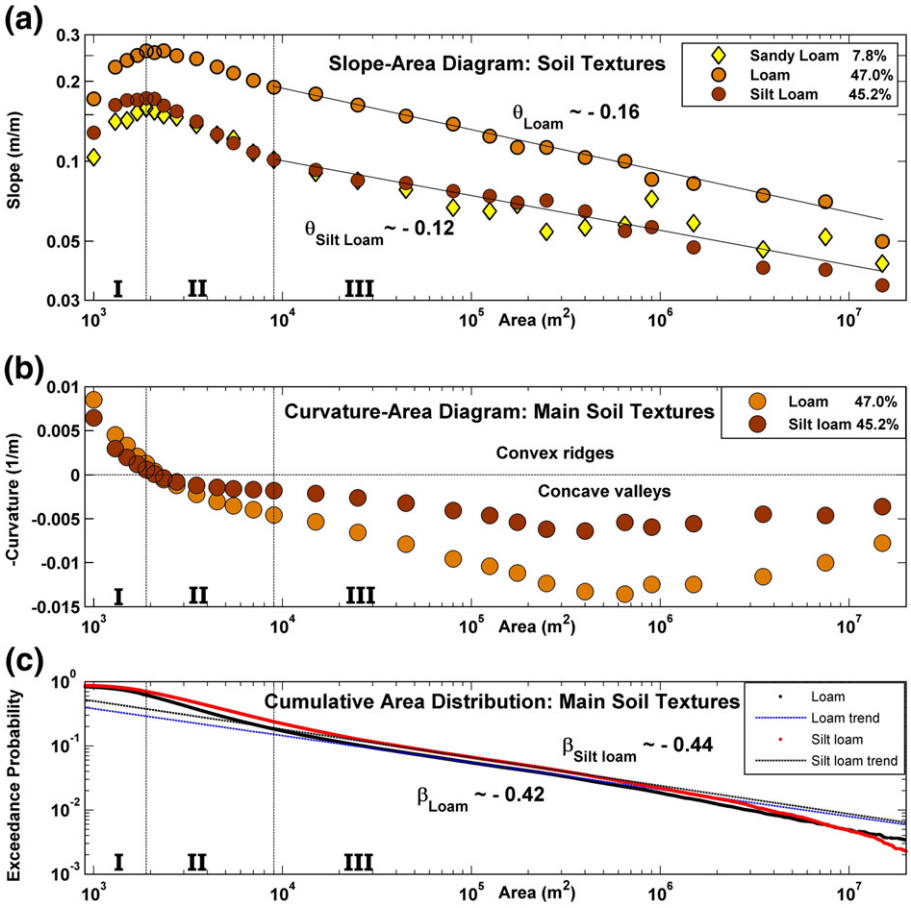

Fig. 7. (a) Slope–area (S–A) relation; (b) curvature–area (C–A) relation and; (c) cumulative area distribution (CAD) of the types of soil textures in the URS basin.

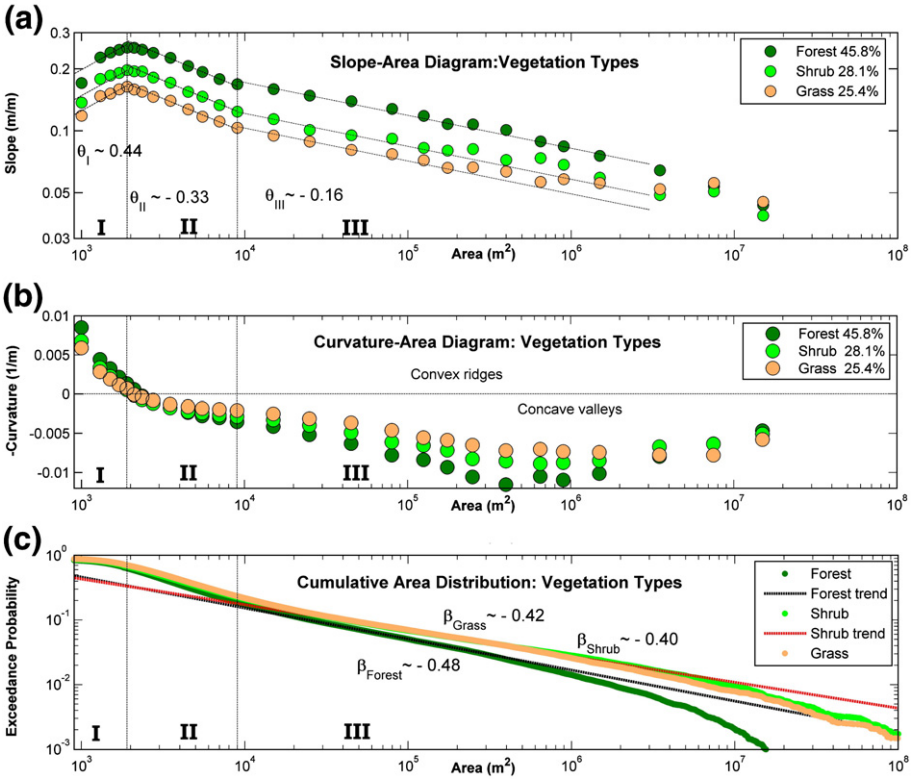

Fig. 8. (a) Slope–area (S–A) relation; (b) curvature–area (C–A) relation and; (c) cumulative area distribution (CAD) of the types of vegetation in the URS basin. Note: The trend line for grass is not given in (c) for clarity purpose.

that differences in the type of vegetation do not influence the nonlinear dependence of geomorphic processes to A and S within a given scaling region, but do influence the transport efficiency coefficient K in (Eq. (1)). This theoretical interpretation emphasizes the conclusions of Dietrich and Perron (2006) and suggests that same morphologies may exist under different vegetations, but with slightly different scaling properties.

In the curvature–area (C–A) diagram (Fig. 8b), forests show the highest ridge divergence and valley convergence, followed by shrublands. Grasslands have the least divergent ridges and least convergent valleys. We attribute this pattern to variations in the steepness index, k. The larger k observed in forests implies a higher rate of change in gradient along hillslopes and valleys, leading to higher values of curvature across the forest landscape (Eq. (5)). In contrast, a smaller k in grasslands would lead to a lower rate of slope change with area indicating a lower curvature on hillslopes and valleys.

A consistent observation in all C–A relations is that, the properties of the land surface that plot steeper throughout all three regions of the S–A relation exhibit a higher degree of ridge divergence in region I, and a higher degree of convergence in regions II and III of their corresponding C–A relations than other groups. This can be clearly observed in Kcc–Tps, loam–silt loam, and forest–shrub–grass comparisons (Figs. 6b, 7b, and 8b). Typically, regardless of the surface property examined, the C–A relations show fairly constant gradients in regions I and II; while in region III, they dip down remarkably and reach a global maximum around 5×10^5 m^2. Beyond this point, curvature gradually increases with area. Interestingly, this global maximum in the binned average C–A data does not have a signature in the S–A relation of the basins.

The CADs of all groups follow a power-law function beginning with drainage areas slightly larger than the area threshold for region III in the respective S–A relations. The power-law exponents of the CAD for grasses and shrubs are very close and well within the universal range reported in the literature, while the trees exponent is slightly larger (Fig. 8c).

4.2.2. Interactive comparisons of land surface properties and the URS topography

The analyses presented thus far focused on examining the impacts of different types (e.g., tree, grass, shrub) of a given surface property (e.g., vegetation) on some catchment geomorphic descriptors. In reality, landscape morphology emerges from the intertwine linkages among lithology, soils, and vegetation through numerous biotic and abiotic processes forced by climate and tectonics. Here, we propose to compare the S–A relations of different types (e.g., forest, grass, shrub) of a selected landscape surface property (e.g., vegetation) within a domain where the other two types of land surface property remain fixed (e.g., soil: loam; lithology: Kcc). We do this by constraining the coverage of the study domain to the overlapping regions of the two fixed types of land surface property (e.g., soil: loam; lithology: Kcc), and plotting the S–A relation of the different types of the third land surface property observed within that domain (e.g., vegetation: forest, grass, shrub). A combination of these different types of land surface properties will be called a land surface group (LSG) in the remainder of the paper. In this section, we only used Kcc and Tps lithologies in the URS basin. These lithologies underlie approximately 78% of the entire basin area, are away from local faults located in the upper portions of the basin, and their S–A relations do not visually present any significant disparities (Fig. 6a).

First, we investigate the influence of soil texture followed by vegetation. In the left panel of Fig. 9, we plot the S–A relations for types of soil textures only within the basin areas characterized by Kcc geology; and grass (Fig. 9a), shrub (Fig. 9c), and forest (Fig. 9e) vegetation, respectively. In the right panel, the same is repeated for Tps lithology (Fig. 9b, d, f). In the legend of each figure, the areas corresponding to each type of soil textures are given in parenthesis as percentages of the entire basin area. Soil percentages in the Kcc lithology are relatively stable under different types of vegetation, but significantly variable in Tps. Consistently in each LSG, loam has steeper slopes than sandy and silt loam, especially for areas less than 10^6 m^2.

Next, the S–A relations for different types of vegetation, grouped with respect to Tps and Kcc lithology, are presented in Fig. 10a and b, respectively. Here, to examine the impact of grouping with respect to lithology only, we did not include the soil groups in the analysis. A clear separation exists between forests, shrublands, and grasslands in Kcc where each type of vegetation has approximately equal proportions within the domain as reported in the legend of the figure. Because of a strong control of elevation on the spatial distribution of the types of vegetation, forests largely dominate the Tps areas located at higher elevations than Kcc. Lower percentages of shrubs and grasses over Tps lithology, lead to highly fluctuating S–A trends for these types of vegetation in Fig. 10b. It is likely that this causes a mixing of slopes of shrubs and forests in region I. Regardless of lithology and elevation, grasses register the shallowest slopes in the basin.

In order to incorporate the soil groups, next we used the Kcc lithology, because of its moderate slopes and approximately equal percentages of soil texture and types of vegetation. The S–A relations are plotted for forests, grasses, and shrubs located on loam (Fig. 11a), silt loam (Fig. 11b), and sandy loam (Fig. 11c), all within the Kcc lithology. Regardless of soil texture, the binned average slope values increase in the grass, shrub, and forest order very consistently in a wide range of drainage areas plotted. As drainage area grows higher than ~10 km^2, the separation becomes less evident because of the decreasing number of data points within each bin.

Figs. 6–11 clearly illustrate the differences in the S–A regions analyzed in relation to landscape lithology, soils, and vegetation. The question that arises here is: which of the LSGs are more influential on the observed landscape morphology as quantified by the S–A relation in this paper? To address this question, we first calculate, for each LSG, the mean landscape slope within all three regions of the S–A relation individually. Then, for LSGs having two identical and one different type of land surface properties, we quantify the impact of the third land surface property by subtracting the mean slopes for each S–A region of the comparing pairs. These differences are used for relative comparisons of types of land surface properties on landscape morphology. In this comparison, we assume that the greater the slope difference between the two types of land surface properties (e.g., forest–grass or loam–silt loam), the higher the impact of that land surface property (e.g., vegetation or soil) on landscape evolution.

To quantify the significance of these results, we test the hypothesis that the mean of the slopes in each S–A region is statistically different ($\alpha=0.01$ using Student's t-test) between any two selected LSGs, having only one type of property different and other two identical. Any LSG occupying lesser coverage than 0.5% of the URS basin is excluded from the analysis. Because large differences in sample sizes of the pairing LSGs, and high variations in slope values over a range of drainage areas in small sample sizes lead to ambiguous results. Statistical comparisons are reported in Table 1. The first column presents the LSGs compared in each row with a heading that specifically identifies the compared types of land surface property. In the subsequent columns, mean slopes and slope differences are reported for S–A regions I, II, and III, respectively. Except one comparison, examining forest–grass difference in silt loam and Tps lithology, all other comparisons are statistically significant at $\alpha=0.01$.

We summarized the results of Table 1 in Fig. 12 by plotting the means of the slope differences for the comparison of each type of land surface property. In Fig. 12, the LSG composed of Loam–Tps–Forest is excluded due to the proximity of this LSG to the resistant rocks and fault activity to avoid any inequalities in the forcing for

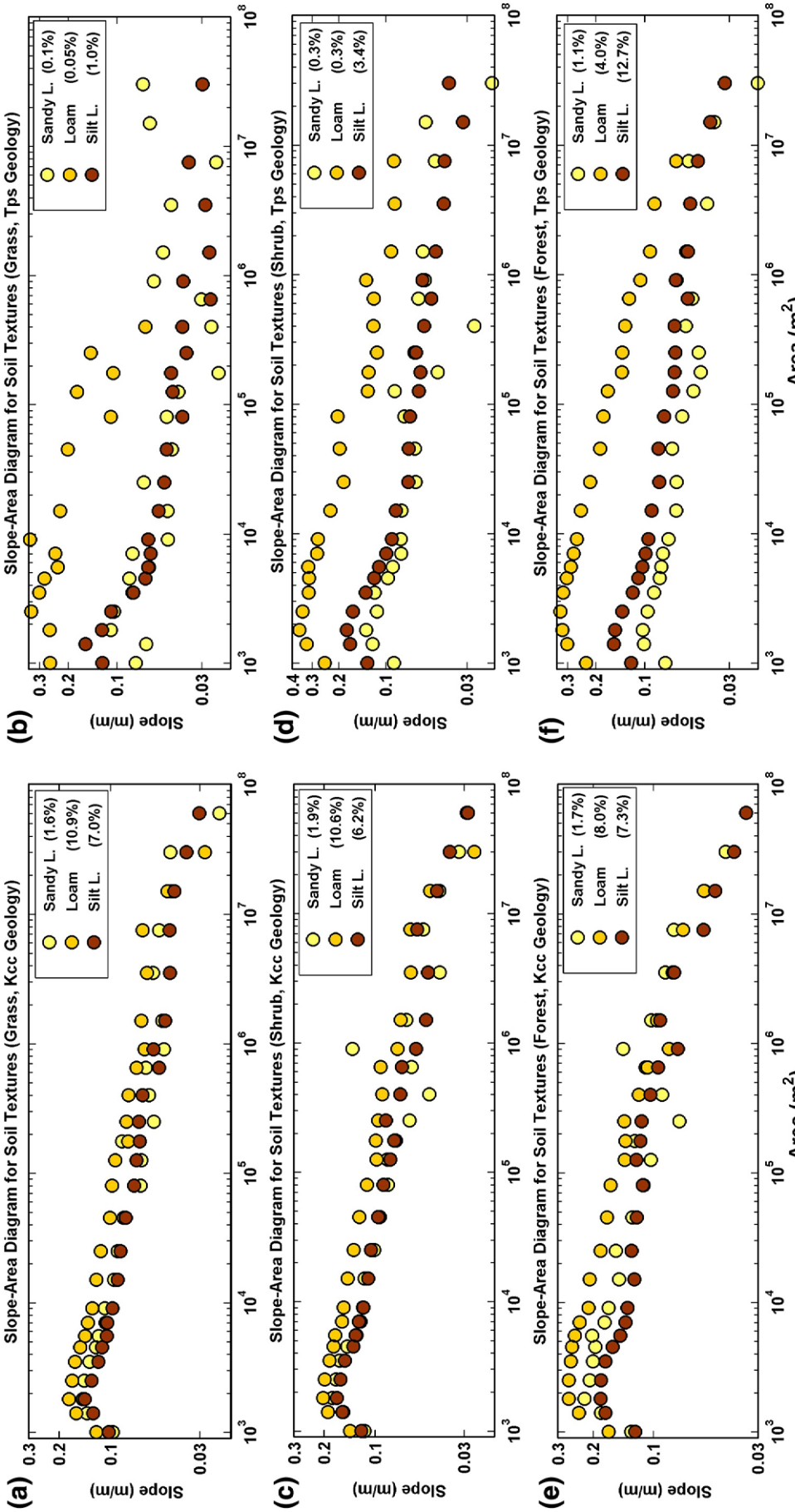

Fig. 9. Slope–area (S–A) plots of the types of soil textures with respect to the same type of vegetation and geologic unit in the URS basin: (a) grass and Kcc; (b) grass and Tps; (c) shrub and Kcc; (d) shrub and Tps; (e) forest and Kcc; (f) forest and Tps.

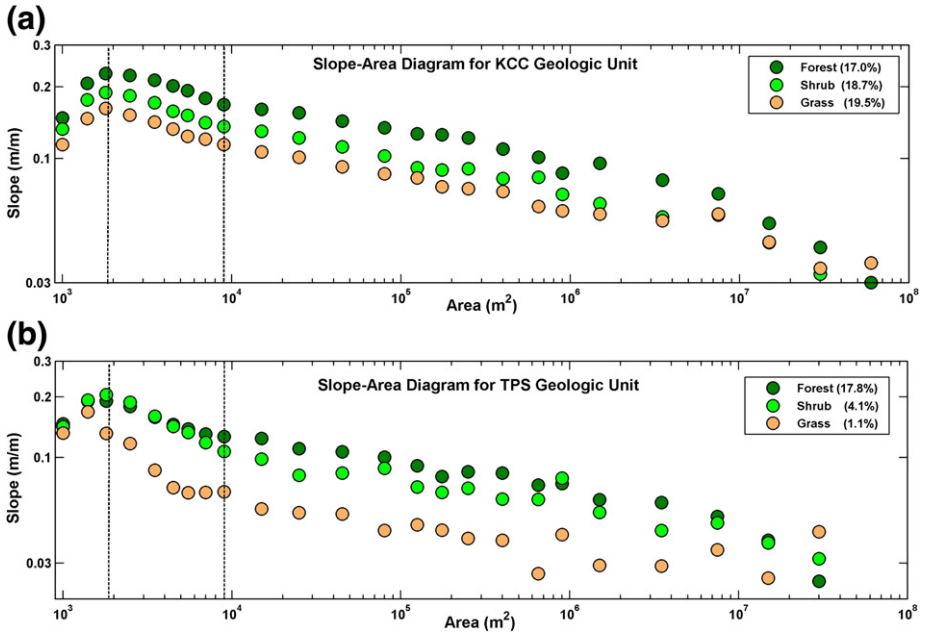

Fig. 10. Slope–area (S–A) plots of the types of vegetation for two dominant geologic units in the URS basin: (a) Kcc; (b) Tps.

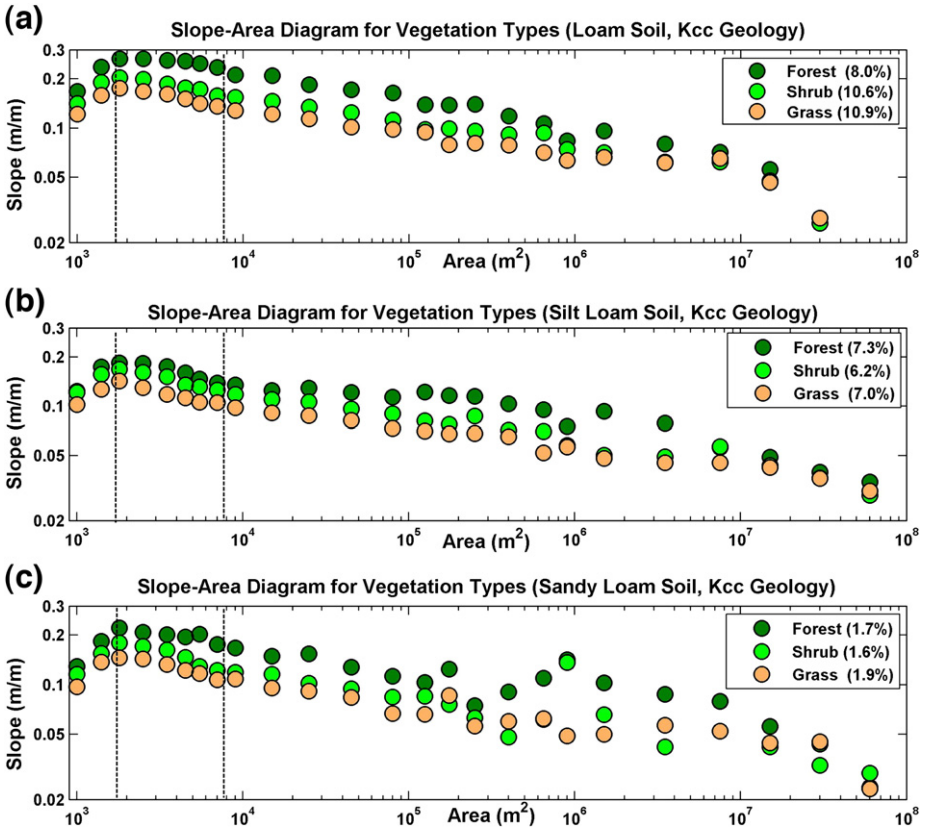

Fig. 11. Slope–area (S–A) plots of the types of vegetation for Kcc geologic unit in different types of soil texture: (a) loam; (b) silt loam; (c) sandy loam.

topographic development. Fig. 12 clearly suggests that on hillslopes (region I) a change in the type of soil texture (loam to silt loam) and vegetation (forest to grass) has the highest influence on slope steepness, followed by shrub to grass and forest to shrub comparisons. In region I, the least impact on the difference in mean slope is observed in the lithology comparison (Fig. 6a). In regions II and III, the leading impact of forest to grass and loam to silt loam change on slope difference continued, with the former moving up in the rank. Interestingly, change in lithology from Kcc to Tps gradually became more influential in the S–A relation in regions II and III. Shrub to grass and forest to grass changes had a lower impact, though significant statistically.

Table 1
Statistical comparison of mean slopes in the slope–area relation of different land surface groups (LSG).

Land surface group (LSG)	Average slope (m/m)			Average slope (m/m)			Average slope (m/m)		
	Region I[a]			Region II[a]			Region III[a]		
Shrub–grass	LSG. I[b]	LSG. II[b]	Diff[c].	LSG. I	LSG. II	Diff.	LSG. I	LSG. II	Diff.
Loam Kcc shrub–loam Kcc grass	0.166	0.144	0.023	0.186	0.157	0.029	0.133	0.112	0.021
Silt loam Kcc shrub–silt loam Kcc grass	0.141	0.119	0.022	0.147	0.118	0.029	0.103	0.086	0.017
Silt loam Tps shrub–silt loam Tps grass	0.154	0.131	0.023	0.135	0.083	0.052	0.078	0.052	0.026
Forest–shrub	LSG. I	LSG. II	Diff.	LSG. I	LSG. II	Diff.	LSG. I	LSG. II	Diff.
Loam Kcc forest–loam Kcc shrub	0.202	0.166	0.036	0.258	0.186	0.072	0.187	0.133	0.054
Silt loam Kcc forest–silt loam Kcc shrub	0.148	0.141	0.007	0.169	0.147	0.022	0.124	0.103	0.021
Silt loam Tps forest–silt loam Tps shrub	0.137	0.154	−0.016	0.120	0.135	−0.015	0.085	0.078	0.007
Forest–grass	LSG. I	LSG. II	Diff.	LSG. I	LSG. II	Diff.	LSG. I	LSG. II	Diff.
Loam Kcc forest–loam Kcc grass	0.202	0.144	0.059	0.258	0.157	0.100	0.187	0.112	0.075
Silt loam Kcc forest–silt loam Kcc grass	0.148	0.119	0.029	0.169	0.118	0.051	0.124	0.086	0.037
Silt loam Tps forest–silt loam Tps grass	0.137	0.131	0.007[d]	0.120	0.083	0.037	0.085	0.052	0.032
Kcc–Tps	LSG. I	LSG. II	Diff.	LSG. I	LSG. II	Diff.	LSG. I	LSG. II	Diff.
Loam Kcc forest–loam Tps forest[e]	0.202	0.268	−0.066	0.258	0.314	−0.056	0.187	0.219	−0.031
Silt loam Kcc forest–silt loam Tps forest	0.148	0.137	0.011	0.169	0.120	0.048	0.124	0.085	0.039
Silt loam Kcc shrub–silt loam Tps shrub	0.141	0.154	−0.012	0.147	0.135	0.012	0.103	0.078	0.025
Silt loam Kcc grass–silt loam Tps grass	0.119	0.131	−0.012	0.118	0.083	0.035	0.086	0.052	0.034
Loam–silt loam	LSG. I	LSG. II	Diff.	LSG. I	LSG. II	Diff.	LSG. I	LSG. II	Diff.
Loam Kcc forest–silt loam Kcc forest	0.202	0.148	0.054	0.258	0.169	0.089	0.187	0.124	0.063
Loam Kcc shrub–silt loam Kcc shrub	0.166	0.141	0.025	0.186	0.147	0.039	0.133	0.103	0.030
Loam Kcc grass–silt loam Kcc grass	0.144	0.119	0.024	0.157	0.118	0.039	0.112	0.086	0.026
Loam Tps forest[e]–silt loam Tps forest	0.268	0.137	0.131	0.314	0.120	0.193	0.219	0.085	0.134

[a] Drainage area bands covered by the S–A scaling regions are region I: 900–1900 m^2, region II: 1900–9000 m^2, and region III: 9000–200,000 m^2, respectively.
[b] LSG. I and LSG. II, aliases for the LSGs explained in the first column in their respective order.
[c] Diff. refers to slope differences between LSG. I and LSG. II.
[d] Not statistically significant at $\alpha = 0.05$.
[e] May be affected by the resistant units and local fault activity.

5. Discussions

5.1. Measures of catchment morphology

Analysis of the DEMs and field observations suggest that the development and maintenance of perennial channels require greater drainage areas than those observed where the S–A turnover occurs (Montgomery and Dietrich 1989, 1992; Istanbulluoglu et al., 2003). Consistent with this notion, others showed that the log–log linear portion of the CAD begins with a change in the gradient of the S–A relation usually in region III of the S–A relation of fluvial basins (Ijjasz-Vasquez and Bras, 1995) or in region IV in landslide dominated valleys (McNamara et al., 2006). In our analysis in the SNWR and the URS basins, the log–log linear portion of the CADs begins with drainage areas slightly larger than the area threshold for region III in their corresponding S–A relations, without a pronounced break in the gradient of the S–A relation. Subtle separations occur among the CADs for different surface conditions within a basin as well. The CAD of a region with steeper slopes plots below the CAD of shallower slopes, meaning that the exceedance probability of a given area is higher for regions with lower slopes. This suggests that the land surface properties may influence the constant of the power-law distribution, while the scaling exponent of the distribution remains close to 0.43.

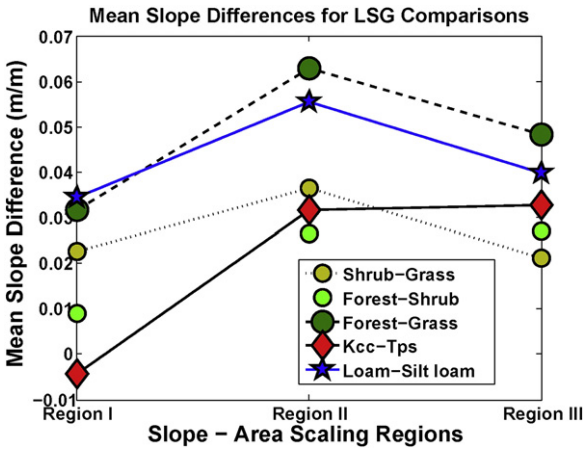

Fig. 12. The comparison of the mean slope differences for different land surface groups.

The C–A relations used in this paper reveal two important features. The first of these is a change in the sign of curvature with drainage area that approximately corresponds to the S–A turnover point. This is consistent with the view that the location of the valley head corresponds to a transition from divergent to convergent morphology (Montgomery and Foufoula-Georgiou, 1993). The second interesting observation is a global maximum in the C–A relation within the concave portion of the landscape. Interestingly, the drainage area range corresponding to this point does not seem to have a detectable imprint in the S–A relation. Because the S–A relation illustrates how slopes change along the landscape profile, following the local flow direction, absence of a clear signature of maximum convergence on the S–A relation suggests that the maximum point arguably results from, first an initial increase in planform curvature with drainage area, and a subsequent decrease leading to the point of maximum curvature. In the URS where valleys are relatively small, this may indicate valley narrowing downslope of the valley head, followed by widening after reaching the maximum convergence. This would certainly require a process-based explanation in relation to the observed surface properties of the landscape. For example, impacts of transitions among geomorphic zones with growing drainage area, such as colluvial–bedrock–alluvial channel transition or migrating headcuts, will need to be examined in the landscape to understand the observed C–A trends. We keep this topic, however, for future investigations.

In aspect- and elevation-controlled semi-arid ecosystems, we found close associations between catchment morphology and its underlying lithology, soil, and vegetation cover. These land surface properties were found to impact slope steepness, the valley head position, and the beginning of perennial channels on the landscape. In the SNWR sites, the mesic north-facing slopes are found to be typically steeper with planar morphology in comparison to xeric south-facing

slopes, which are shallower and more dissected. The S–A and C–A relations are statistically significant (tested for $\alpha = 0.01$ and $\alpha = 0.05$) in the majority of the plotted data (Fig. 5). The S–A model provides a simple but intuitive way to explain these observed differences. The opposing hillslopes in the SNWR site drain into east–west flowing main channels, where the long-term local rate of erosion in both aspects are expected to be identical, and equal to the lowering rate of the main channel. In Eq. (3), S is inversely proportional to K; therefore, under a constant D, steeper north-facing slopes for a given drainage area would imply a lower K (less active wash erosion). Conversely, shallower south-facing slopes would imply a higher K (more active wash erosion) to maintain a constant D. Under the lack of wash erosion, the steeper and planar north-facing slopes suggest dominance of transport by soil creep. These observations imply a strong ecosystem control on landscape morphology.

In soil-mantled landscapes, fluvial erodibility and hillslope diffusivity in the generic slope–area model (Eq. (3)) are determined by soil mechanical and hydrological properties as related to soil texture, functional types and dynamics of vegetation, and other biotic activities such as bioturbation and animal burrowing (e.g., Dietrich et al., 2003). In arid and semi-arid regions, hydrology is strongly dictated by spatial patterns and connectivity of vegetation between the bare and vegetated patches of the landscape (e.g., Gutiérrez-Jurado et al., 2007; Mayor et al., 2008). As such, in savanna ecosystems with grass cover (e.g., Juniper pine-grass in Fig. 1c), hillslope runoff, sediment, and nutrient fluxes are often lower than shrublands (e.g., Fig. 1d), with interconnected bare soil patches and higher rates of overland flow (Abrahams et al., 1998; Neave and Abrahams 2002; Wainwright et al., 2000). These views have led to the development of conceptual models of ecosystem function differentiating the landscapes between resource conserving, such as savannas, versus non-conserving (fragmented shrubby landscapes) in semi-arid climate regimes (Davenport et al., 1998; Reid et al., 1999; Wilcox et al., 2003; Saco et al., 2007). Consistent with these views, the south-facing slopes in the SNWR sites, subject to more erosive runoff, could maintain long-term rates of erosion equal to base-level fall with shallower slopes, while more resistant north-facing slopes, with lower runoff potentials, require higher hillslope gradients to keep up with base-level fall, largely with soil creep transport, which is often much less efficient in removing sediment than transport by soil wash. In a recent paper, Gutiérrez-Jurado et al. (2007) reported differences in soil moisture between the north- and south-facing slopes in the headwater slopes of the Lower SLF (Fig. 1b), illustrating the resource conserving and non-resource conserving roles, respectively. These observations suggest an ecohydrological control on landscape evolution facilitated by hillslope aspect in the SNWR basins.

Application of the S–A model is also helpful for understanding the local dynamics of the tectonic setting. In Fig. 3a, the Higher SLF basins plot the steepest, and the Lower SLF basin plots the shallowest slopes as a function of area (difference up to twofold), while the S–A relations of the PF and the heterogeneous basins appear between the two. Theoretically in Eq. (3), a steeper slope for a given A would suggest a higher D or a smaller K. Under the same lithology, climate, and with approximately 200 m of altitude difference, we do not expect the erodibility parameter K to vary significantly between the Higher and Lower SLF basins. Some regional geology maps show a local fault (Silver Creek Fault) that traverses the foothills of the Ladron Peak (Nimick, 1986). It is conceivable that the steep morphology of the Higher SLF basins results from a local base-level dynamics rather than lithology and elevation.

Similar arguments maybe made to interpret the S–A separation observed among different types of vegetation on identical lithology and soil texture in the URS basin (Fig. 11). Greater thresholds of erosion, associated with the soil-binding effects of roots and the additive roughness of understory cover as well as arguably enhanced rates of soil infiltration under semi-arid vegetation (e.g., Cerdà, 1998), could naturally lead to lower rates of overland flow and runoff erosion. Several studies have demonstrated, although at field-scale experiments, lower rates of runoff erosion in forested landscapes than shrublands and grasslands (under uniform slopes for all ecosystems) in the southwest USA (e.g., Allen and Breshears, 1998; Johansen et al., 2001; Breshears et al., 2003), which could theoretically lead to the observed separation in the vegetation S–A relations. Forest ecosystems are typically characterized by higher long-term rates of soil creep because of the bioturbation processes that actively take place in forests (Black and Montgomery, 1991; Nash, 1994; Roering et al., 2002). Despite this, however, in the nonlinear soil creep equation of Roering et al. (1999), forested hillslopes bear greater critical hillslope gradients for threshold slopes than unvegetated slopes or a laboratory sand pile (Roering et al., 1999, 2001). This indicates that soil slips would occur under shallower hillslope gradients on bare or sparsely vegetated surfaces with interconnected bare patches than forested basins, offering an explanation for the steeper maximum slopes observed at the valley head position of the forests in the URS basin than shrubs and grasses (Figs. 8 and 11).

The S–A relations of soil textures clearly show that all other land surface properties being identical, loam slopes are steeper than silt loam slopes in the URS basin (Fig. 9). This provides a landscape-scale evidence for higher erodibility for silt loam than loam. Some empirical data exists to support this finding. Field studies conducted to estimate the erodibility factor for the Universal Soil Loss Equation (USLE) demonstrate that all other soil properties being unchanged (e.g. soil organic matter), soil erodibility decreases as soil texture approaches from silt loam to loam in the soil texture triangle (Wischmeier and Mannering, 1969). Field studies conducted to parameterize the runoff erosion component of the WEPP model also report similar trends for the rill erodibility coefficient of the WEPP model (Flanagan and Livingston, 1995).

The comparisons among LSGs suggest that different types of soil texture, vegetation, and lithological units have a detectable impact on the observed morphology of the basin (Table 1, Fig. 12). Interestingly, changes in soil texture (from loam to silt loam) and vegetation (from forest to grass) have shown the greatest increase on slope steepness in the URS basin, while the impact of lithological change gained significance in the fluvial regions of the S–A relation (regions II and III). The growing influence of lithological change on slopes towards downstream maybe related to changes in the hydrological regime and biological processes tied to sediment thickness on rock with increasing drainage area, modulating both the rates and efficiency of soil creep (Yoo et al., 2005; Roering, 2008), and runoff erosion (Istanbulluoglu, 2009). As such, as the drainage area gets larger, one expects increased local soil loss, leading to thinner regolith, partially exposed bedrock, or development of alluvial soils where sediment carrying capacity of the system drops. As a result, lithological differences within the landscape, especially if the parent material responds differentially to fluvial processes, will likely manifest themselves in the channel profile geometry. The primary rock types for Kcc and Tps are fine- and medium-grained mixed clastic rock, respectively. As a secondary type of rock, Kcc, includes coal, and Tps includes tuff. According to Green and Jones (1997), the Tps lithology has a tertiary type of rock consisting of limestone, sand, and clay. Based on this, it is plausible that fluvial erodibility of Tps would be slightly higher than Kcc. This interpretation is consistent with the S–A relation of different lithologies (Figs. 6a and 12). Kcc slopes plot steeper than Tps with increasing drainage area, implying a lower erodibility than that of Tps according to the S–A model (Eq. (3)). Earlier research has extensively discussed the role of bedrock on the form of channel profiles (Stock and Montgomery, 1999; Whipple, 2004; Stock et al., 2005) and cross-sectional geometry (Montgomery, 2004; Finnegan et al., 2005), however, little is known about its relative role on catchment morphology within the hillslope–valley–channel continuum.

Despite the consistencies of our results both aspect- and elevation-controlled ecosystems, we realized that our data sets were relatively coarse. Recently, in a headwater catchment (~0.1 km^2) located in the Lower SLF, compared the S–A and C–A relations derived from a 1-m LiDAR (Light Detection and Ranging) DEM and the 10-m IfSAR DEM used in this study. Their comparison did not reveal any significant differences between the S–A diagrams of the two products, albeit considerable statistical variations in the C–A relations were found.

In interpreting our results, it is crucial to recognize that a great deal of mismatch occurs among the time scales of rock, soil, and vegetation dynamics of the land surface. Rocks act as the parent material for soils, and over geomorphically significant time scales, they may be considered fixed in space. In our study basins, the alluvial fan deposits of the Sierra Ladrones Formation (SLF) are easily older than ~1 Ma in the SNWR sites, and the rocks in the URS basin are arguably at least several millions (or possibly more) years old. Soils on the other hand develop over much smaller time scales through interactions with vegetation and climate (e.g., Monger and Bestelmeyer, 2006; Buxbaum and Vanderbilt, 2007). The separations in the S–A and C–A relations conditioned on different types of soil and vegetation raise an important question: Are the observed differences in slope caused by modern aspect- and elevation-induced trends in soils and vegetation patterns, or do relict influences occur in the observed topographic patterns? This question is critical to advance our understanding of climate change impacts on landscape morphology and rates of erosion. We did not further discuss the role of lithology and soil on the observed topography. We do not have a detailed historical view of the rocks and soils in the region, and soil development and age could be highly dependent on geomorphic position on the landscape. We briefly addressed the vegetation and erosion history of the region, because some historical data make this possible.

5.2. Climate fluctuations and its impacts on vegetation, rates of erosion, and topography

In the southwestern United States, the late Pleistocene climate (the last ice age, 30,000–13,000 yr BP) was wetter and cooler than in the Holocene (last 11,000 years) and today. During that time, current desert elevations (300–1700 m) were covered with piñon-juniper–oak woodlands, while higher elevations, including the elevation range of the URS basin, contained spruce–fir, mixed-conifer, and subalpine forests (Betancourt et al., 1990; Thompson et al., 1993). The transition from glacial to interglacial periods around 12,000 yr BP triggered major ecological changes in the region, including migration of sparse piñon woodlands to higher elevations, replacing conifer forests; and the establishment of desert vegetation at the present-day elevations. The modern climate regime was developed ~4000 years ago, which led to creosote bush establishment in the SNWR (Holmgren et al., 2007) and shrubs and grasses in the lower elevations of the URS.

Strong evidence shows that this climate transition and vegetation change enhanced erosion activity in the region. For example, arroyo formation and cut and fill cycles first began around 8000 yr BP, and intensified in the past 4000 years (Waters and Haynes, 2001). Vegetation–erosion interactions under a fluctuating climate regime with wet and dry cycles are believed to have significantly contributed to the arroyo cycles in the southwest United States (e.g., Cooke and Reeves, 1976; Bull, 1997; Istanbulluoglu and Bras, 2006). Rapid erosion still continues in the region with contemporary sediment yields closely matching the late Holocene rates on hillslopes and slightly larger in valleys (Gellis et al., 2004; Bierman et al., 2005).

These observations lead us to the following hypothesis that: the observed differences in the landscape morphology in relation to land surface groups result from climate fluctuations that are capable of replacing vegetation functional types. This hypothesis implies that the S–A differences between forest–shrub–grass comparisons have emerged during the alternating wet–dry periods when forests in the low elevations of the URS basin were replaced by shrubs and grasses; and the trees in the south-facing slopes of the SNWR sites are replaced by shrubs. This hypothesis can be explained conceptually using the S–A model. If erosion is in balance with soil generation by weathering—shown to hold for at least the late Holocene and today, in the Rio Puerco Basin, north of the Rio Salado (Bierman et al., 2005)—then landscapes adjust such that for a given drainage area, all sites erode at similar rates. This implies that steeper slopes will be needed to erode forested landscapes that may have lower runoff erosion potential than shrublands and grasslands (under uniform slopes for all ecosystems) (e.g., Allen and Breshears, 1998; Johansen et al., 2001; Breshears et al., 2003), in approximately at the same rates as grasslands. The same explanation holds for the desert elevations in the SNWR site, where north- and south-facing aspects are lowered by a master channel.

Our hypothesis does not limit the time scale of climate fluctuations to the last glacial–interglacial cycle (or late Pleistocene–Holocene climate transition). Since the beginning of the Pleistocene, glacial–interglacial fluctuations, driven by the Milankovitch cycles with ~20 to ~100 kyr periods, have prevailed with varying frequencies, and have resulted in enhanced rates of sedimentation worldwide (Zhang et al., 2001). For as long as the plants existed in this region, we expect that during each dry period, mesic vegetations developed in the north-facing slopes of desert elevations and upper elevations of mountains, while xeric species dominated the south-facing slopes as well as low elevation bands of pronounced topographies. These proposed long-term periodic shifts in vegetation patterns and differential erosion/deposition events may also contribute to explaining the observed valley asymmetry in the southwest and western United States (e.g., Istanbulluoglu et al., 2008).

6. Conclusions

Associations between observed morphologies of several semi-arid catchments in the southwestern United States and the land surface properties (underlying rock type, soils, and vegetation) were examined. In the study catchments, aspect and elevation had a strong control on the observed vegetation patterns. Basin morphologies were quantified by the following catchment geomorphic descriptors: the slope–area relation, the curvature–area relation, and the cumulative distribution of catchment drainage areas. To facilitate comparisons of the impacts of land surface properties, land surface groups (LSGs) were developed in which all, except one type of land surface property, were kept identical. Examining the differences in the catchment geomorphic descriptors with respect to various LSGs, relative impacts of changes in lithology, soils, and vegetation types were quantified.

Our analysis revealed dependencies between LSGs and landscape morphology. Earlier research studied the impacts of soils and geology within this context (Hancock, 2005; Cohen et al., 2008). In this study, the influence of functional types of vegetation detected on observed topography, provide some initial understanding of the potential impacts of life on catchment organization. This finding also emphasizes the critical role of climate in the landscape processes. We suggest that climatic fluctuations that are capable of replacing vegetation communities could lead to highly amplified hydrological and geomorphic responses. Consistent with this idea, the continuing high sediment losses from many semi-arid basins in the southwestern United States have been related to the Holocene climate change that caused the re-organization of regional vegetation (Bierman et al., 2005). These findings provide testable hypothesis, and underscore the necessity of numerical models as conceptual frameworks to integrate the dynamics of climate and vegetation with Earth surface processes and examine linkages between ecosystem processes and the evolution of landscapes.

Acknowledgements

This work was supported by NSF grant EAR-0819923. We acknowledge Sevilleta LTER for the IfSAR data. We thank J. Bruce J. Harrison and H. A. Gutiérrez-Jurado for their collaboration. We also thank two anonymous reviewers and John D. Vitek for their constructive and helpful comments in improving the manuscript.

References

Abrahams, A.D., Li, G., Krishnan, C., Atkinson, J.F., 1998. Predicting sediment transport by interrill overland flow on rough surfaces. Earth Surface Processes and Landforms 23, 1087–1099.

Allen, C.D., Breshears, D.D., 1998. Drought-induced shift of a forest–woodland ecotone: rapid landscape response to climate variation. Proceedings of the National Academy of Sciences 95, 14839–14842.

Betancourt, J.L., Van Devender, T.R., Martin, P.S. (Eds.), 1990. Packrat Middens: The Last 40,000 Years of Biotic Change. University of Arizona Press, Tucson, Arizona.

Bierman, P.R., Reuter, J.M., Pavich, M., Gellis, A.C., Caffee, M.W., Larsen, J., 2005. Using cosmogenic nuclides to contrast rates of erosion and sediment yield in a semi-arid, arroyo-dominated landscape, Rio Puerco Basin, New Mexico. Earth Surface Processes and Landforms 30, 935–953.

Black, T.A., Montgomery, D.R., 1991. Sediment transport by burrowing mammals, Marin County, California. Earth Surface Processes and Landforms 16 (2), 163–172.

Bogaart, P.W., Troch, P.A., 2006. Curvature distribution within hillslopes and catchments and its effect on the hydrological response. Hydrology and Eart System Sciences 10, 925–936.

Bogaart, P.W., Tucker, G.E., de Vries, J.J., 2003. Channel network morphology and sediment dynamics under alternating periglacial and temperate regimes: a numerical simulation study. Geomorphology 54, 257–277.

Branson, F.A., Shown, L.M., 1989. Contrasts of vegetation, soils, microclimates, and geomorphic processes between north- and south-facing slopes on Green Mountain near Denver, Colorado. United States Geological Survey, Department of the Interior, Water-Resources Investigations Report, pp. 89–4094.

Breshears, D.D., Whicker, J.J., Johansen, M.P., Pinder, J.E., 2003. Wind and water erosion and transport in semi-arid shrubland, grassland and forest ecosystems: quantifying dominance of horizontal wind-driven transport. Earth Surface Processes and Landforms 28, 1189–1209.

Bruning, 1973. Origin of the Popotosa Formation, north-central Socorro County, New Mexico. Ph.D. dissertation, New Mexico Institute of Mining and Technology, Socorro, NM.

Bull, W.B., 1997. Discontinuous ephemeral streams. Geomorphology 19 (3–4), 227–276.

Burnett, B.N., Meyer, G.A., McFadden, L.D., 2008. Aspect-related microclimatic influences on slope forms and processes, northeastern Arizona. Journal of Geophysical Research 113, F03002.

Buxbaum, C.A.Z., Vanderbilt, K., 2007. Soil heterogeneity and the distribution of desert and steppe plant species across a desert–grassland ecotone. Journal of Arid Environments 69, 617–632.

Casadei, M., Dietrich, W.E., Miller, N.L., 2003. Testing a model for predicting the timing and location of shallow landslide initiation in soil-mantled landscapes. Earth Surface Processes and Landforms 28, 925–950.

Caylor, K.K., Manfreda, S., Rodriguez-Iturbe, I., 2005. On the coupled geomorphological and ecohydrological organization of river basins. Advances in Water Resources 28, 69–86.

Cerdà, A., 1998. The influence of geomorphological position and vegetation cover on the erosional and hydrological processes on a Mediterranean hillslope. Hydrological Processes 12, 661–671.

Chamberlin, R.M., Kues, B.S., Cather, S.M., Barker, J.M., McIntosh, W.C., 1994. Mogollon Slope, West-Central New Mexico and East-Central Arizona. Forty-Fifth Annual Field Conference. New Mexico Geological Society, Socorro. 335 pp.

Churchill, R.R., 1981. Aspect-related differences in badlands slopes morphology. Annals of the Association of American Geographers 71 (3), 374–388.

Cohen, S., Willgoose, G., Hancock, G., 2008. A methodology for calculating the spatial distribution of the area–slope equation and hypsometric integral within a catchment. Journal of Geophysical Research 113, F03027.

Collins, D.B.G., Bras, R.L., Tucker, G.E., 2004. Modeling the effects of vegetation–erosion coupling on landscape evolution. Journal of Geophysical Research 109, F03004.

Cooke, R.U., Reeves, R.W., 1976. Arroyos and Environmental Change in the American South-West. Clarendon, Oxford, U.K.

Davenport, D.W., Breshears, D.D., Wilcox, B.P., Allen, C.D., 1998. Viewpoint: sustainability of piñon-juniper ecosystems—a unifying perspective of soil erosion thresholds. Journal of Range Management 51, 231–240.

Dickie-Peddie, W.A., 1993. New Mexico Vegetation: Past, Present, and Future. University of New Mexico Press, Albuquerque. 244 pp.

Dietrich, W.E., Perron, J.T., 2006. The search for a topographic signature of life. Nature 439, 411–418.

Dietrich, W.E., Bellugi, D.G., Sklar, L.S., Stock, J.D., Heimsath, A.M., Roering, J.J., 2003. Geomorphic transport laws for predicting the form and dynamics. In: Wilcock, P., Iverson, R. (Eds.), Prediction in Geomorphology. AGU, Washington, D.C, pp. 103–132.

Ebel, B.A., Loague, K., Dietrich, W.E., Montgomery, D.R., Torres, R., Anderson, S.P., Giambelluca, T.W., 2007a. Near-surface hydrologic response for a steep, unchanneled catchment near Coos Bay, Oregon: 1. Sprinkling experiments. American Journal of Science 307, 678–708.

Ebel, B.A., Loague, K., Vanderkwaak, J.E., Dietrich, W.E., Montgomery, D.R., Torres, R., Anderson, S.P., 2007b. Near-surface hydrologic response for a steep, unchanneled catchment near Coos Bay, Oregon: 2. Physics-based simulations. American Journal of Science 307, 709–748.

Finnegan, N.J., Roe, G., Montgomery, D.R., Hallet, B., 2005. Controls on the channel width of rivers: implications for modeling fluvial incision of bedrock. Geology 33 (3), 229–232.

Flanagan, D.C., Livingston, S.J. (Eds.), 1995. WEPP User Summary. NSERL Report No. 11, National Soil Erosion Research Laboratory. West Lafayette, Indiana.

Gabet, E.J., 2000. Gopher bioturbation: field evidence for non-linear hillslope diffusion. Earth Surface Processes and Landforms 25, 1419–1428.

Gabet, E.J., 2003. Sediment transport by dry ravel. Journal of Geophysical Research 108 (B1), 2049.

Gabet, E.J., Dunne, T., 2003. A stochastic sediment delivery model for a steep Mediterranean landscape. Water Resources Research 39 (9), 1237.

Gabet, E.J., Reichman, O.J., Seabloom, E.W., 2003. The effects of bioturbation on soil processes and sediment transport. Annual Review of Earth and Planetary Sciences 31, 249–273.

Gasparini, N.M., Tucker, G.E., Bras, R.L., 2004. Network-scale dynamics of grain-size sorting: implications for downstream fining, stream-profile concavity, and drainage basin morphology. Earth Surface Processes and Landforms 29, 401–421.

Gasparini, N.M., Whipple, K.X., Bras, R.L., 2007. Predictions of steady state and transient landscape morphology using sediment-flux-dependent river incision models. Journal of Geophysical Research 112, F03S09.

Gellis, A.C., Pavich, M.J., Bierman, P.R., Clapp, E.M., Ellevein, A., Aby, S., 2004. Modern sediment yield compared to geologic rates of sediment production in a semi-arid basin, New Mexico: assessing the human impact. Earth Surface Processes and Landforms 29, 1359–1372.

Green, G.N., Jones, G.E., 1997. The Digital Geologic Map of New Mexico in ARC/INFO Format. U.S. Geological Survey Open-File Report OFR 97-0052. U.S. Geological Survey, Denver, Colorado.

Gutiérrez-Jurado, H.A., Vivoni, E.R., Harrison, J.B.J., Guan, H., 2006. Ecohydrology of root zone water fluxes and soil development in complex semiarid rangelands. Hydrological Processes 20, 3289–3316.

Gutiérrez-Jurado, H.A., Vivoni, E.R., Istanbulluoglu, E., Bras, R.L., 2007. Ecohydrological response to a geomorphically significant flood event in a semiarid catchment with contrasting ecosystems. Geophysical Research Letters 34, L23S25.

Hadley, R.F., 1961. Some effects of microclimate on slope morphology and drainage basin development. United States Geological Survey, Department of the Interior. Geological Survey Research 1961, B32–B34.

Hancock, G.R., 2005. The use of digital elevation models in the identification and characterization of catchments over different grid scales. Hydrological Processes 19, 1727–1749.

Holmgren, C.A., Norris, J., Betancourt, J.L., 2007. Inferences about winter temperatures and summer rains from the late Quaternary record of C_4 perennial grasses and C_3 desert shrubs in the northern Chihuahuan Desert. Journal of Quaternary Science 22 (2), 141–161.

Howard, A.D., 1980. Thresholds in river regimes. In: Coates, D.R., Vitek, J.D. (Eds.), Thresholds in Geomorphology. Allen & Unwin, London, pp. 227–258.

Ijjasz-Vasquez, E.J., Bras, R.L., 1995. Scaling regimes of local slope versus contributing area in digital elevation models. Geomorphology 12, 299–311.

Ijjász-Vásquez, E.J., Bras, R.L., Moglen, G.E., 1992. Sensitivity of a basin evolution model to the nature of runoff production and to initial conditions. Water Resources Research 28 (10), 2733–2741.

Istanbulluoglu, E., 2009. An eco-hydro-geomorphic perspective to modeling the role of climate in catchment evolution. Geography Compass 3 (3), 1151–1175.

Istanbulluoglu, E., Bras, R.L., 2005. Vegetation-modulated landscape evolution: effects of vegetation on landscape processes, drainage density, and topography. Journal of Geophysical Research 110, F02012.

Istanbulluoglu, E., Bras, R.L., 2006. On the dynamics of soil moisture, vegetation, and erosion: implications of climate variability and change. Water Resources Research 42, W06418.

Istanbulluoglu, E., Tarboton, D.G., Pack, R.T., Luce, C., 2003. A sediment transport model for incision of gullies on steep topography. Water Resources Research 39 (4), 1103.

Istanbulluoglu, E., Yetemen, O., Vivoni, E.R., Gutiérrez-Jurado, H.A., Bras, R.L., 2008. Ecogeomorphic implications of hillslope aspect: Inferences from analysis of landscape morphology in central New Mexico. Geophysical Research Letters 35, L14403.

Johansen, M.P., Hakonson, T.E., Breshears, D.D., 2001. Post-fire runoff and erosion from rainfall simulation: contrasting forests with shrublands and grasslands. Hydrological Processes 15, 2953–2965.

Kirkby, M.J., 1971. Hillslope process–response models based on the continuity equation. In: Brunsden, D. (Ed.), Slopes, Form and Process. Special Publication 3. Institute of British Geographers, London, pp. 15–30.

Lancaster, S.T., Grant, G.E., 2006. Debris dams and the relief of headwater streams. Geomorphology 82, 84–97.

Lavee, H., Imeson, A.C., Sarah, P., 1998. The impact of climate change on geomorphology and desertification along a Mediterranean-arid transect. Land Degradation and Development 9, 407–422.

Mayor, A.G., Bautista, S., Small, E.E., Dixon, M., Bellot, J., 2008. Measurement of the connectivity of runoff source areas as determined by vegetation pattern and topography: a tool for assessing potential water and soil losses in drylands. Water Resources Research 44, W10423.

McKean, J.A., Dietrich, W.E., Finkel, R.C., Southon, J.R., Caffee, M.W., 1993. Quantification of soil production and downslope creep rates from cosmogenic ^{10}Be accumulations on a hillslope profile. Geology 21 (4), 343–346.
McMahon, D.R., 1998. Soil, landscape and vegetation interactions in a small semi-arid drainage basin: Sevilleta National Wildlife Refuge. M.S. thesis, New Mexico Institute of Mining and Technology, Socorro, NM.
McNamara, J.P., Ziegler, A.D., Wood, S.H., Vogler, J.B., 2006. Channel head locations with respect to geomorphologic thresholds derived from a digital elevation model: a case study in northern Thailand. Forest Ecology and Management 224, 147–156.
Moglen, G.E., Bras, R.L., 1995a. The effect of spatial heterogeneities on geomorphic expression in a model of basin evolution. Water Resources Research 31 (10), 2613–2623.
Moglen, G.E., Bras, R.L., 1995b. The Importance of spatially heterogeneous erosivity and the cumulative area distribution. Geomorphology 12, 173–185.
Molina, A., Govers, G., Cisneros, F., Vanacker, V., 2009. Vegetation and topographic controls on sediment deposition and storage on gully beds in a degraded mountain area. Earth Surface Processes and Landforms 34, 755–767.
Monger, H.C., Bestelmeyer, B.T., 2006. The soil-geomorphic template and biotic change in arid and semi-arid ecosystems. Journal of Arid Environments 65, 207–218.
Montgomery, D.R., 2001. Slope distributions, threshold hillslopes, and steady-state topography. American Journal of Science 301, 432–454.
Montgomery, D.R., 2004. Observations on the role of lithology in strath terrace formation and bedrock channel width. American Journal of Science 304, 454–476.
Montgomery, D.R., Dietrich, W.E., 1989. Source areas, drainage density and channel initiation. Water Resources Research 25 (8), 1907–1918.
Montgomery, D.R., Dietrich, W.E., 1992. Channel initiation and the problem of landscape scale. Science 255, 826–830.
Montgomery, D.R., Foufoula-Georgiou, E., 1993. Channel network source representation using digital elevation models. Water Resources Research 29 (12), 3925–3934.
Montgomery, D.R., Dietrich, W.E., 1994. Landscape dissection and drainage area–slope thresholds. In: Kirkby, M.J. (Ed.), Process Models and Theoretical Geomorphology. John Wiley & Sons, New York, pp. 221–246.
Montgomery, D.R., Dietrich, W.E., 2002. Runoff generation in a steep, soil-mantled landscape. Water Resources Research 38 (9), 1168.
Montgomery, D.R., Abbe, T.B., Buffington, J.M., Peterson, N.P., Schmidt, K.M., Stock, J.D., 1996. Distribution of bedrock and alluvial channels in forested mountain drainage basins. Nature 381, 587–589.
Montgomery, D.R., Dietrich, W.E., Heffner, J.T., 2002. Piezometric response in shallow bedrock at CB1: implications for runoff generation and landsliding. Water Resources Research 38 (12), 1274.
Murray, A.B., Paola, C., 2003. Modelling the effect of vegetation on channel pattern in bedload rivers. Earth Surface Processes and Landforms 28, 131–143.
Nash, D.B., 1994. Effective sediment-transporting discharge from magnitude–frequency analysis. Journal of Geology 102 (1), 79–95.
Neave, M., Abrahams, A.D., 2002. Vegetation influences on water yields from grassland and shrubland ecosystems in the Chihuahuan Desert. Earth Surface Processes and Landforms 27, 1011–1020.
New Mexico Bureau of Geology and Mineral Resources, 2003. Geologic Map of New Mexico, 1:500,000. New Mexico Bureau of Geology and Mineral Resources.
Nimick, K.G., 1986. Geology and structural evolution of the east flank of the Ladron Mountains, Socorro County, New Mexico. M.S. Thesis, University of New Mexico, Albuquerque, NM.
Pierce, K.L., Colman, S.M., 1986. Effect of height and orientation (microclimate) on geomorphic degradation rates and processes, late-glacial terrace scarps in central Idaho. Geological Society of America Bulletin 97, 869–885.
Reid, K.D., Wilcox, B.P., Breshears, D.D., MacDonald, L., 1999. Runoff and erosion in a piñon-juniper woodland: influence of vegetation patches. Soil Science Society of America Journal 63, 1869–1879.
Rinaldo, A., Dietrich, W.E., Rigon, R., Vogel, G.K., Rodriguez-Iturbe, I., 1995. Geomorphological signatures of varying climate. Nature 374, 632–635.
Rodríguez-Iturbe, I., Ijjász-Vásquez, E.J., Bras, R.L., Tarboton, D.G., 1992. Power law distributions of discharge mass and energy in river basins. Water Resources Research 28 (4), 1089–1093.
Roering, J.J., 2008. How well can hillslope evolution models "explain" topography? Simulating soil transport and production with high-resolution topographic data. Geological Society of America Bulletin 120 (9–10), 1248–1262.
Roering, J.J., Kirchner, J.W., Dietrich, W.E., 1999. Evidence for nonlinear, diffusive sediment transport on hillslopes and implications for landscape morphology. Water Resources Research 35 (3), 853–870.
Roering, J.J., Kirchner, J.W., Sklar, L.S., Dietrich, W.E., 2001. Hillslope evolution by nonlinear creep and landsliding: an experimental study. Geology 29 (2), 143–146.
Roering, J.J., Almond, P., Tonkin, P., McKean, J., 2002. Soil transport driven by biological processes over millennial time scales. Geology 30 (12), 1115–1118.
Saco, P.M., Willgoose, G.R., Hancock, G.R., 2007. Eco-geomorphology of banded vegetation patterns in arid and semi-arid regions. Hydrology and Earth System Sciences 11, 1717–1730.
Schmidt, K.M., Montgomery, D.R., 1995. Limits to relief. Science 270, 617–620.
Schmidt, K.M., Montgomery, D.R., 1996. Rock mass strength assessment for bedrock landsliding. Environmental and Engineering Geoscience 2, 325–338.
Sklar, L., Dietrich, W.E., 1998. River longitudinal profiles and bedrock incision models: stream power and the influence of sediment supply. In: Tinkler, K.J., Wohl, E.E. (Eds.), Rivers over Rock: Fluvial Processes in Bedrock Channels. AGU, Washington D.C., pp. 237–260.
Smith, B.J., 1978. Aspect-related variations in slope angle near Béni Abbès, western Algeria. Geografiska Annaler 60 A (3–4), 175–180.
Snow, R.S., Slingerland, R.L., 1987. Mathematical modeling of graded river profiles. Journal of Geology 95, 15–33.
Soil Survey Staff, 1994. State Soil Geographic Database (STATSGO) data users guide. USDA Natural Resources Conservation Service Misc. Publ. 1492. U.S. Government Printing Office, Washington, DC, pp. 88–1036.
Stock, J.D., Montgomery, D.R., 1999. Geologic constraints on bedrock river incision using the stream power law. Journal of Geophysical Research 104 (B3), 4983–4993.
Stock, J.D., Montgomery, D.R., Collins, B.D., Dietrich, W.E., Sklar, L., 2005. Field measurements of incision rates following bedrock exposure: implications for process controls on the long profiles of valleys cut by rivers and debris flows. Geological Society of America Bulletin 117 (11–12), 174–194.
Tarboton, D.G., Bras, R.L., Rodriguez-Iturbe, I., 1992. A physical basis for drainage density. Geomorphology 5, 59–76.
Tarolli, P., Dalla Fontana, G., 2009. Hillslope-to-valley transition morphology: new opportunities from high resolution DTMs. Geomorphology 113, 47–56.
Thompson, R.S., Whitlock, C., Bartlein, P.J., Harrison, S.P., Spaulding, W.G., 1993. Climatic changes in the western United States since 18,000 yr BP. In: WrightJr. Jr., H.E., Kutzbach, J.E., WebbIII III, T., Ruddiman, W.F., Street-Perrott, F.A., Bartlein, P.J. (Eds.), Global Climates since the Last Glacial Maximum. University of Minnesota Press, St. Paul, MN, pp. 468–513.
Torres, R., Dietrich, W.E., Montgomery, D.R., Anderson, S.P., Loague, K., 1998. Unsaturated zone processes and the hydrologic response of a steep, unchanneled catchment. Water Resources Research 34 (8), 1865–1879.
Tucker, G.E., Slingerland, R., 1997. Drainage basin responses to climate change. Water Resources Research 33 (8), 2031–2047.
Tucker, G.E., Bras, R.L., 1998. Hillslope processes, drainage density, and landscape morphology. Water Resources Research 34 (10), 2751–2764.
Vivoni, E.R., Moreno, H.A., Mascaro, G., Rodriguez, J.C., Watts, C.J., Garatuza-Payan, J., Scott, R., 2008. Observed relation between evapotranspiration and soil moisture in the North American monsoon region. Geophysical Research Letters 35, L22403.
Vivoni, E.R., Aragón, C.A., Malczynski, L., Tidwell, V.C., 2009. Semiarid watershed response in central New Mexico and its sensitivity to climate variability and change. Hydrology and Earth System Sciences 13, 715–733.
Vogelmann, J.E., Howard, S.M., Yang, L., Larson, C.R., Wylie, B.K., Van Driel, N., 2001. Completion of the 1990s national land cover data set for the conterminous United States from Landsat Thematic Mapper data and ancillary data sources. Photogrammetric Engineering and Remote Sensing 67, 650–662.
Wainwright, J., Parsons, A.J., Abrahams, A.D., 2000. Plot-scale studies of vegetation, overlandflow and erosion interactions: case studies from Arizona and New Mexico. Hydrological Processes 14, 2921–2943.
Waters, M.R., Haynes, C.V., 2001. Late Quaternary arroyo formation and climate change in the American Southwest. Geology 29 (5), 399–402.
Whipple, K.X., 2004. Bedrock rivers and the geomorphology of active orogens. Annual Review of Earth and Planetary Sciences 32, 151–185.
Whipple, K.X., Tucker, G.E., 2002. Implications of sediment-flux-dependent river incision models for landscape evolution. Journal of Geophysical Research 107 (B2), 2039.
Wilcox, B.P., Breshears, D.D., Allen, C.D., 2003. Ecohydrology of a resource-conserving semiarid woodland: effects of scale and disturbance. Ecological Monographs 73 (2), 223–239.
Wischmeier, W.H., Mannering, J.V., 1969. Relation of soil properties to its erodibility. Soil Science Society of America Journal 33, 131–137.
Willgoose, G., 1994. A physical explanation for an observed area–slope–elevation relationship for catchments with declining relief. Water Resources Research 30 (2), 151–159.
Willgoose, G., Bras, R.L., Rodriguez-Iturbe, I., 1991. A coupled channel network growth and hillslope evolution model 1. Theory. Water Resources Research 27 (7), 1671–1684.
Wobus, C., Whipple, K.X., Kirby, E., Snyder, N., Johnson, J., Spyropolou, K., Crosby, B., Sheehan, D., 2006. Tectonics from topography: procedures, promise, and pitfalls. In: Willett, S.D., Hovius, N., Brandon, M.T., Fisher, D.M. (Eds.), Tectonics, Climate and Landscape Evolution. GSA, Boulder, CO, pp. 55–74.
Yoo, K., Amundson, R., Heimsath, A.M., Dietrich, W.E., 2005. Process-based model linking pocket gopher (Thomomys bottae) activity to sediment transport and soil thickness. Geology 33 (11), 917–920.
Zhang, P., Molnar, P., Downs, W.R., 2001. Increased sedimentation rates and grain sizes 2–4 Myr ago due to the influence of climate change on erosion rates. Nature 410, 891–897.